# Testing a novel method for protein-assembly based vaccine construction

**MD Nasir Uddin Badal**

**Master's thesis**

**Tampere University**

**Faculty of Medicine and Health Technology**

**June 2019**

# Master's thesis

| | | |
|---|---|---|
| **Place** | : | Tampere University<br>Faculty of Medicine and Health Technology (MET) |
| **Author** | : | MD Nasir Uddin Badal |
| **Title** | : | Testing a novel method for protein-assembly based vaccine construction |
| **Supervisor** | : | Minna Hankaniemi, PhD |
| **Pages** | : | 55 |
| **Reviewers** | : | |
| **Date** | : | June 2019 |

# Abstract

Vaccination is thought to be the most effective and versatile component against infectious diseases. Emerging infectious diseases and limited effectiveness of currently available influenza vaccine can cause a serious public health threat to people worldwide. Millions of people are affected in yearly influenza outbreaks and more than 250,000 lives are lost annually. This study aimed to create a universal influenza vaccine prototype that will be cost effective, easy to produce, would provide long-term immunity and effectiveness against multiple strains of influenza and would be highly immunogenic. This kind of vaccine can be possibly formed by conjugating conserved M2e antigen and Norovirus-like particle (NoV-VLP) using two peptide tags (Spy-Tag and K-Tag) and Spyligase protein.

The extracellular domain of influenza A virus matrix protein-2 (M2e) was aimed to use as target antigen. M2e antigen was fused with a peptide tag (K-Tag) for the formation of isopeptide bond with another peptide tag (Spy-Tag) with the help of Spyligase. Spyligase is the essential enzyme to form covalent bond between K-Tag-Spy-Tag, that was expressed in BL21 Star DE3 *E. coli* strain. After complete purification of Spyligase using immobilized metal affinity chromatography (IMAC) method, 86 mg/l of Spyligase protein was obtained with >95% purity. Spy-Tag was genetically fused with Noro VLP so that, VLP could be decorated and conjugated with K-Tagged antigen. Spy Noro VLP was expressed in Hi-5 insect cells and purified with tangential flow filtration (TFF), 30 % sucrose cushion pelleting and anion exchange chromatography. Estimated yield from this purification was 133 mg/l with >95% purity. WT Noro VLP was purified using the same protocol as Spy Noro VLP and yield was 3.8 mg/l with >95% or >50% purity. Hydrodynamic diameter for Spy Noro VLP was 51 nm and for >95% pure WT Noro VLP and >50% pure WT Noro VLP were 53 nm and 32 nm respectively.

Spy-Tagged Noro virus like particle, K-Tagged antigen and Spyligase were mixed together and incubated at 4ºC for 24 hours. SDS-PAGE and western blot analysis showed the isopeptide bond formation and successful conjugation of two peptide tag.

**Keywords:** Infectious Disease, Influenza, Vaccine, Norovirus, Virus like particle, isopeptide bond, Spy-Tag-K-Tag, Spyligase

# Preface

This Master's thesis has done in the Protein Dynamics research group at the faculty of Medicine and health technology in Tampere University.

First of all, I would like to express my heartfelt gratitude to Almighty ALLAH for creating me, guiding me, giving me strength to work in the mysterious field of Science. I am very glad to the international student selection board of Tampere University for giving me the study opportunity and grants for my master's degree.

I am very grateful to our group leader Vesa Hytönen for guiding me from the very beginning of my study in Tampere and for his excellent teaching and providing me an opportunity to work in his research group. I want to thank my respectable supervisor Minna Hankaniemi, for her valuable guidance, patience and practical teaching in the whole way of my thesis. I always feel lucky to have an opportunity to work under her supervision. This is now time to thank my colleague and friend Vili Lampinen for his enormous help and teaching lab work.

I am very thankful to Olli Laitinen and Juha Määttä for informative support and encouraging me during my thesis work. Niila Saarinen deserves thanks from me for nice sporting and refreshing Pelimannet events. Thanks a lot, to Latifeh Azizi for technical support during my thesis work. Exclusively, I am very delighted to have such nice working environment and all nice members of Protein dynamics group. I feel Niklas Kähkönen as a man of light for his excellency about all lab equipment's and found strength when he was in my side. I want to thank Merja Jokinen and Ulla Kiiskinen for giving me all technical support. Thanks to all group members to provide me warm friendship and sharing knowledge whenever I needed.

Finally, I want to remember my late father and my beloved mother all my siblings and friends and teachers for supporting me and encouraging me throughout my study abroad. Again, thanks to ALLAH for giving me such a wonderful family.

June 2019, Tampere, Finland.

MD Nasir Uddin Badal

# Contents

# Table of figures

# Abbreviations

| | |
|---|---|
| Spy Noro VLP | Spy-Tagged Noro virus like particle |
| VLP | Virus like particle |
| BSA | Bovine serum albumin |
| DLS | Dynamic light scattering |
| Dpi | Days post infection |
| FBS | Fetal bovine serum |
| HA | Hemagglutinin protein (Influenza) |
| IMAC | Immobilized metal affinity chromatography |
| IPTG | Isopropyl β-D-1thiogalactopyranoside |
| LB | Lysogeny broth |
| NA | Neuraminidase protein (Influenza) |
| WT Noro VLP | Wild Type Noro virus like particle |
| M2e | Ectodomain of influenza matrix protein-2 |
| M1 | Influenza matrix protein-1 |
| NP | Influenza nucleocapsid protein |
| NS | Influenza non-structured protein |
| OD | Optical density |
| ORF | Open reading frame |
| PBS | Phosphate-buffered saline |
| PCT | Phosphate-citrate-trimethylamine-N-oxide buffer |
| PEG | Polyethylene glycol |
| RNP | Ribonucleoprotein |
| SDS-PAGE | Sodium dodecyl sulfate polyacrylamide gel electrophoresis |
| TBS | Tris-buffered saline |
| WB | Western blotting |
| MHC | Major histocompatibility complex |
| TFF | Tangential flow filtration. |

# 1 Introduction

Influenza, structurally simple but highly infectious virus is a threat for the whole world because of its high morbidity and mortality (Bright et al., 2007; Hong et al., 2019; Rossman, et al., 2010). Frequent out bursting and infections with a pandemic potential has been imposing economic burden. By different virus strain of influenza, more than (5-30) % world population are affecting annually, resulting in millions of hospitalizations and thousands of deaths every year (Sautto et al., 2018). Until March 2019, in last six months only in USA 26.3 million people were infected, >289000 people were hospitalized and >31,200 people were dead by influenza infection (Centre for disease control and prevention, 2019). In the last century it was and at present time it is a threat for the people of the world. Devastating consequence from Spanish influenza in 1918 (~50 million deaths), Asian influenza in 1957 (2 million deaths) and Hong Kong influenza in 1968 (One million deaths) is still a fresh painful memory for the mankind (World Health Organization, 2009). There have been almost ten pandemics in the last 300 years that have caused loss of innumerable number of people. From the past experience it could be guessed that, a mild new pandemic could kill millions of people (Osterholm, 2005).

Vaccination is the most cost-effective method for preventing influenza infection and reducing mortality (Kang et al., 2012). Influenza vaccine has been available since last 70 years but still epidemic and pandemic have been occurring by this virus with substantial damages (Valkenburg et al., 2016). Vaccination against influenza infection is the prophylactic countermeasure which target to reduce the burden of influenza. However, current influenza vaccine efficiency is limited due to the antigenic diversity of the virus strains. These vaccines are only active against selected strains and isolates circulating in the environment (Sautto et al., 2018). On the other hand, it is very difficult to guess about the next strain because it is totally uncertain and cannot say anything about the mutation and antigenic shift and drift (Osterholm, 2005). Prediction inaccuracy of circulating viral stain and new reassortment possibility are causes of pandemic outbreaks. To solve this problem it requires an anti-influenza vaccine with an increased protection, high producibility and deployment (Valkenburg et al., 2016).

Most of the currently market available influenza vaccines have been producing targeting the transmembrane glycoprotein HA and NA (Bright et al., 2007; Hong et al., 2019; Rossman et al., 2010). Hypervariability of amino acids of these proteins is responsible for outbreaks of pandemic influenza. Small changes of amino acids due to antigenic shift and drift is enough to

inactivate the current vaccines and loss of protection (Godbey, 2014; Sautto et al., 2018).To overcome this limitation, it is highly needed to produce an effective, broadly reactive universal influenza vaccine which is capable of protecting seasonal as well as newly emerging pre-pandemic strains. Two possible approaches would be targeting conserved sequence which is common in seasonal and pandemic virus and another would be eliciting broader immune response that could confer protection against circulating influenza strains (Sautto et al., 2018).

The extracellular domain of transmembrane influenza protein M2 (M2e) is almost completely conserved among most of the strains of influenza virus and is considered as a strong candidate for the next universal influenza vaccine. Preclinical studies with M2e protein with VLP or without carrier have shown excellent immune response against influenza virus stains (Ebrahimi and Tebianian, 2011). Virus Like particles are the most efficient carrier for virus antigen because of its highly immunogenic nature. VLPs are similar in structure and morphology (Bright et al., 2007; Brune et al., 2016) of native virus but produce without viral genome. In some cases, VLPs have shown eliciting broader immune responses than the whole inactivated virus or recombinant hemagglutinin.(Bright et al., 2007). In a recent scientific report a successful production of influenza vaccine has been described by using HA matrix protein (Hong et al., 2019), here Noro VLP was used as platform for the formation of virus particle.

Noro virus like particles were produced using Hi-5 insect cells and Spyligase protein was expressed in BL21 Star DE3 *E. coli* strain. Purification of VLPs was done using tangential flow filtration (TFF), sucrose cushion pelleting by ultracentrifugation and anion exchange chromatography. Spyligase purification was done using immobilized metal affinity chromatography (IMAC). Spy Noro VLP, Spyligase and K-Tagged antigen were mixed to form the conjugated vaccine particle. Spy-Tagged Noro VLP and K-Tagged M2e antigen formed covalent bond between peptide tags incorporated by Spyligase. Conjugation of M2e antigen and Spy Noro VLP was detected with SDS-PAGE and western blot analysis.

# 2 Review of literature

The research topic of the study was to test a novel method for protein-assembly based vaccine construction. We aimed to produce a universal vaccine targeting the influenza virus M2e matrix protein. Influenza has been a continuous threat since last century, but concrete solution has not been identified yet due to its frequent genetically changing nature. Characteristic features of influenza and conserved target antigens of influenza are mostly clear to researchers. In this section of review all general information about influenza, ongoing research activity against influenza and target antigens will be described. Moreover, peptide tags and their successful application in vaccine production will be reviewed.

## 2.1 Influenza

### 2.1.1 Overview and life cycle

Influenza viruses are commonly flu causing, enveloped, single stranded RNA viruses of the Orthomyxoviridae family (Nayak et al., 2009; Szewczyk et al., 2014). Spherical shaped influenza viruses are about 100-200 nm in diameter (Szewczyk et al., 2014). There are four types of influenza viruses, A, B, C, D, which are responsible for different types of seasonal flu in animals and humans (Centre for disease control and prevention, 2019). Influenza A circulates in human, dogs, pigs, horses and birds (Garcia-Sastre and Medina, 2011) and show various symptoms such as fever, cough, sore throat, malaise within very short 1-3 days post incubation period (Houser and Subbarao, 2015). Virus type A and B together result epidemics in a rate of 5-10% and 15-30% to children and adults respectively (World Health Organisation, 2018). Another recent WHO report shows that about 1 billion people are infected every year, 3-10 million falls on severe illness and 300 000-500 000 people die annually (Krammer et al., 2018). Influenza A virus from Zoonotic sources, sometimes causes pandemics, resulting economic loss with massive mortality. In last century four pandemics occurred due to virus types A and B (Houser and Subbarao, 2015). In contrast virus types C and D responsible for respiratory illness, do not harm humans but causes flu to dogs (Centre for disease control and prevention, 2019).

In composition, influenza viruses are single stranded negative sense RNA virus that have three distinct structural properties. Firstly, hemagglutinin (HA), neuraminidase (NA) and Matrix protein-2 (M2), comprising of virus envelop. Secondly, intermediate matrix protein layer (M1). Thirdly, viral core capsid, comprising of viral ribonucleic protein (vRNP) and viral ribonucleic acid (v RNA) (Nayak et al., 2009).

Additionally, influenza viruses contain eight segmented single stranded negative sense vRNA (except seven in Influenza D), that encode 11-12 (Garcia-Sastre and Medina, 2011) or 11-17 ( Levene and Gaglia, 2018) different viral proteins engaging throughout their life cycle. Among these proteins, N40 is one of the newly discovered proteins transcribed from the PB1 gene segment. An arising new virus particle may happen by simultaneous infection to a cell by two different strain of influenza. Pandemic causing new viruses are thought to evolve by this mechanism in the last 100 years e.g. H5N1 (Garcia-Sastre and Medina, 2011). Nucleic acid sequence of M segment encodes transmembrane protein, M2 ion channel and matrix protein M1 surrounded by phospholipid. Both nuclear export protein NS2 and non-structural protein NS1 are transcribed from the NS segments (Figure 1). Moreover, all protein components of RNA dependent RNA polymerase protein (PB1, PB2 and PA), are expressed from their respective segments. Whereas, N40, PB1-F1 and PB1-F2 are newly discovered proteins that transcribe from PB1 segment. Additionally, Hemagglutinin (HA), neuraminidase (NA) and viral nuclear RNA emerge from their respective genome segments (Garcia-Sastre and Medina, 2011). Two very important aspects of influenza genomes are their ability for rapidly change and to produce multiple proteins that help these viruses to infect quite a broad host group, which may go on to cause epidemics and pandemics with the same virus (Levene and Gaglia, 2018).

Moreover, there are 16 subtypes of influenza HA protein, which can be divided into five groups and two clades. This large variability is one of the biggest hurdles for researchers to make disincentives against influenza (Russell et al., 2008). Scientist are researching against these viruses and different virus strains since last three decades. However, because of the newly emerged strain, influenza is still a major threat around the world for many nations. For example, H5N1 is one of the influenza A virus strain that caused an outbreak in 1997. It was first found in birds, but within short time it circulated into humans and became known as bird flu. Avian influenza antigenic drift and shift are the main reason for considerable change of HA subtypes that have been associated with the emergence of pandemic (Garcia-Sastre and Medina, 2011). Virus stain “2009 H1N1” is an example of antigenic shift and drift and this virus strain can cause pandemic by replacing the previous H1N1 virus strain (Centre for disease control and prevention, 2019).

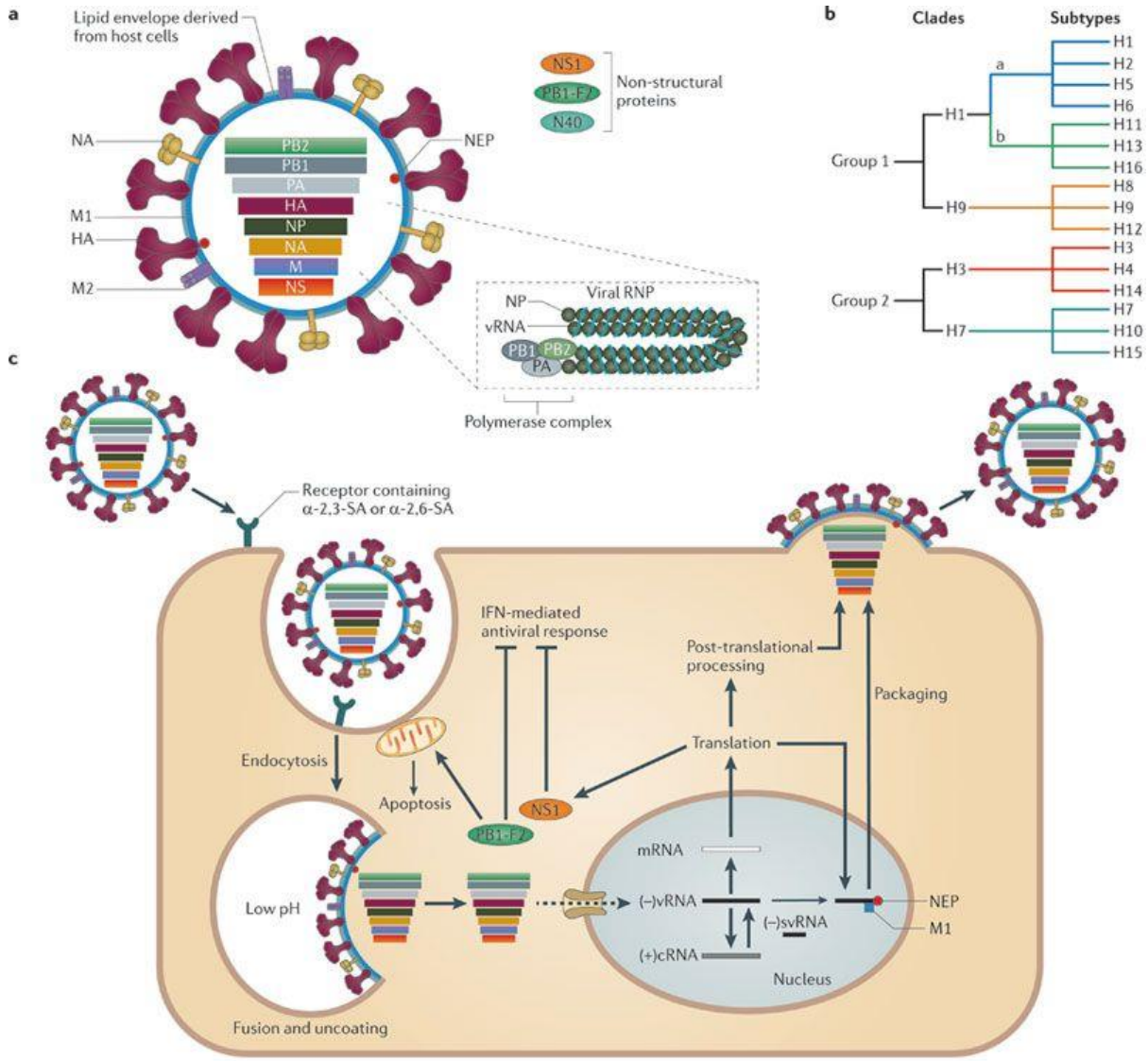


**Figure 1**. Overview of Influenza A virus (Replication and Classification). (**A**) Infectious virus particle. Eight single stranded negative sense virus genome segments in the virus core. HA, NA, M2 transmembrane protein in spike like projections. Non-structural protein NS1 and polymerase complex of RNP. (**B**) Classification of HA which contains 16 subtypes, two clades and five groups. (**C**) Infection to the cells and they first attach by the Hemagglutinin (HA) to the membrane and low pH of the endosome allow to fuse the membrane of the virus and enter the nuclear materials. They incorporate to the host genome and replicate their own genome and transcribe necessary proteins. After having all proteins and nuclear materials they are transported to the cytoplasm from the nucleus through Golgi apparatus and assemble for budding. For fully functioning virus packaging, host membrane is used after that, the NA protein separate the bonds between HA and sialic acid of the host plasma membrane [adapted from (Garcia-Sastre and Medina, 2011)]

### 2.1.2 Attachment and entry

Cell membranes are the complex entity of proteins and lipids, that have indispensable functions in cellular mechanism. These protective liquid-liquid bilayers perform all sorts of

communications with other neighboring cells of tissue, growth factors and hormones ( Meder et al., 2006). In addition, they also hinder attack of the pathogen and resist their easy entry into cell. Lipid rafts are assemblies of lipid, sphingolipid and protein, frequently found in the cell membrane, having a coalesce characteristic, important in cell signaling and membrane trafficking (Chan et al., 2013). Production of virus progeny not only depends on virus machinery but also requires host cellular mechanisms (Chan et al., 2013). Influenza virus production and replication can be divided into sequential events. They are adsorption of virus to cell receptors, entry and uncoating of nuclear materials, replication, synthesis of virus protein, post-translational modification of vRNA protein, assembly and budding of virus (Szewczyk et al., 2014). In the beginning, capsid protein Hemagglutinin (HA) attach to host cell receptor, containing terminal α-2,3 or α-2,6 sialic acid. These sialic acid glycoside bonds differ between human and birds. In case of human, sialic acid carrying α-2,3 glycoside bonds most frequently in trachea whereas, most birds gut has sialic acid with α-2,6 bonds (Garcia-Sastre and Medina, 2011). Sialic acid with α-2,3; is a very easy target of influenza virus which also found in some other organ such as eye, of human (Kumlin et al., 2008).

Having attached to cell receptor, virus enters to cell by clathrin-mediated endocytosis. To cleave hemagglutinin by cellular protease, it is important to expose HA protein. Low pH of endosome helps to relax HA, allowing protease to break bonds between receptors and HA protein (Englander and Mayne, 2014). Acidification of endosome also have another function. It opens M2 ion channel and exchange environmental condition and lower the pH of virus capsid. Low pH helps to uncoated host cell and entry of genetic materials to cells (Gannagé et al., 2009). After that, Hemagglutinin is cleaved into HA1 and HA2 that allow peptide conjugation with N-terminal of HA2 and fuse to endosomal membrane (Momose et al., 2002). For replication of the genome and virus protein production, it is necessary to transport RNA into nucleus. Virus RNA surrounded by Nuclear protein (NP) and Nuclear localization signal (NSL) protein finds NP, helps by transport it to cell nucleus (Szewczyk et al., 2014). After entry to nucleus, RNA-dependent RNA polymerase transcribes negative sense RNA into positive sense RNA. During virus replication three types of RNA can be found: negative sense vRNA, positive sense vRNA and small viral RNA which are thought to be generated by transcription until cell bursts (Garcia-Sastre and Medina, 2011). Replication of RNA and protein is simultaneously happened in nucleus and cytoplasm, including other cellular mechanisms such as splicing, capping and transporting to cytoplasm. Virus RNA-dependent RNA polymerase interacts cellular polymerase II that help in cap release from newly produced

mRNA. In addition, M2 and NS2 virus protein helps to transport vRNA proteins to cytoplasm for modification, assembly and budding (Van de Sandt et al., 2012).

### 2.1.3 Virus assembly and release

Prior to virus assembly some post translational modifications of viral proteins are necessary. Among them hemagglutinin and neuraminidase are transported to golgi apparatus for modification and completed by folding in endoplasmic reticulum. After that, hemagglutinin, neuraminidase, M2 proteins arrive to the plasma membrane. Lipid rafts of the cell membrane is promising site for virus assembly. During their transportation, all eight segments form a complex to membrane for assembly. RNA formation and coating is still a mystery, but it is thought that, there is packaging signal in both sides of the genome (Van de Sandt et al., 2012). M1 protein also plays a very important role of virus assembly, moreover Rab11 protein is associated with the complex formation and assembly (Chou et al., 2013). Complete virus particle is attached with sialic acid with Hemagglutinin prior to their cutting off by neuraminidase. Even though, hemagglutinin, neuraminidase and matrix protein 2 (M2) have affinity to sialic acid of membrane, only hemagglutinin binds there. Balance between sialic acid and hemagglutinin bond is very important to produce enough virus progeny (Szewczyk et al., 2014).

## 2.2 Matrix protein-2 as antigen

Frequent outburst, seasonal epidemics and causing of pandemic are reasons of emphasizing to influenza viruses specially influenza A virus research (Cho et al., 2015). Current influenza vaccines are against transmembrane proteins such as hemagglutinin and neuraminidase. It seems that, those are not enough to stop the infection and economic loss (Van Saparoea et al., 2018). Therefore, conserved transmembrane protein of influenza virion matrix protein 2 (M2) is a suitable target for vaccine researchers (Kang et al., 2012). Recent study revealed that, extracellular matrix protein 2 is evolutionarily conserved area and optimistic epitope for producing universal vaccine (Deng et al., 2015). Pre-clinical trial of some vaccines targeting M2 protein already have proved successful protection in animal models (Fiers et al., 2009). It has been reported that M2 antigen with or without carrier is giving excellent results in phase I and II trials that indicate an effective universal vaccine against influenza virus (Ebrahimi and Tebianian, 2011; Łęga et al., 2016).

M2e virus antigen is conserved protein region having homology with all influenza virus types (Łęga et al., 2016).

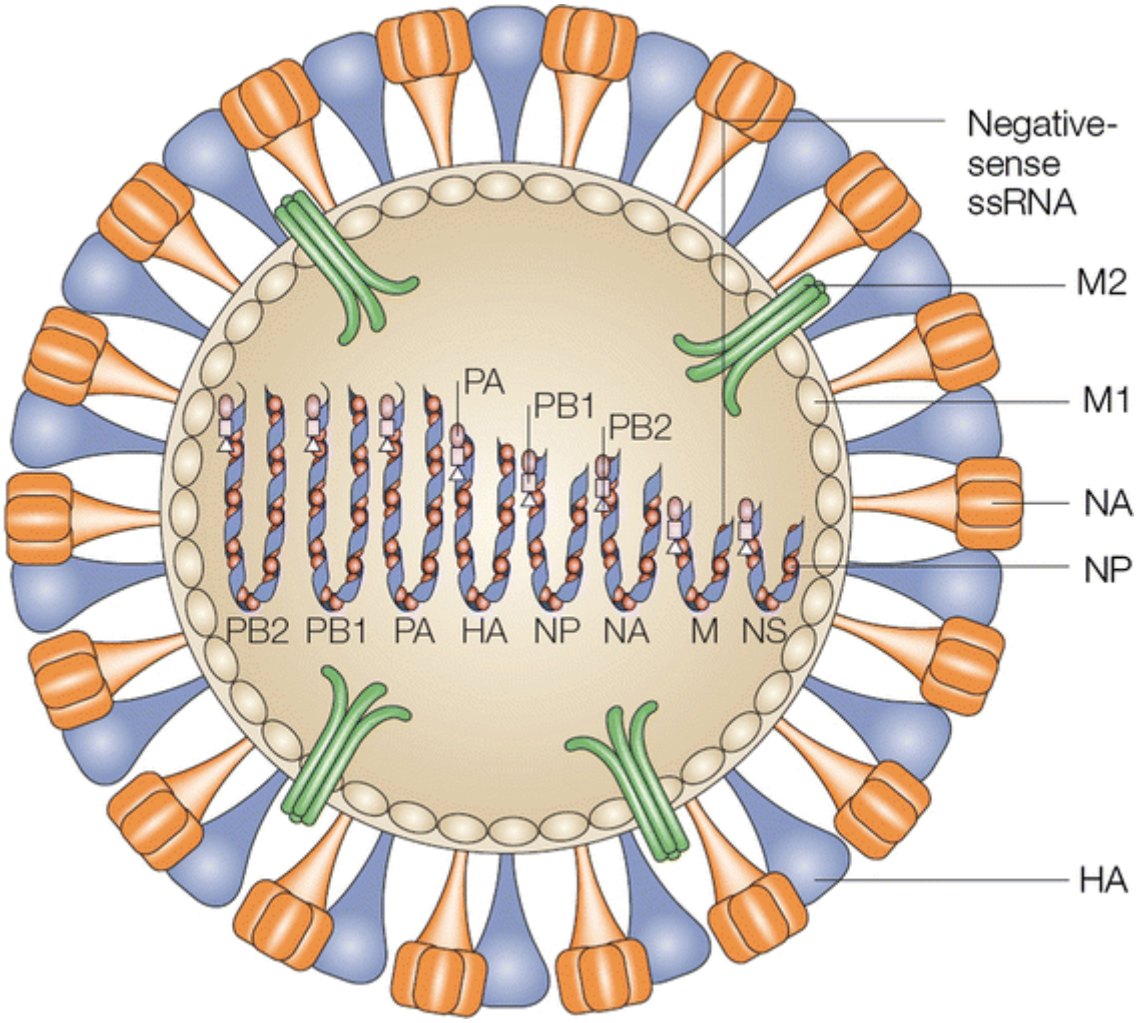


**Figure 2.** Schematic presentation of influenza virus. Outer layer containing three transmembrane protein including hemagglutinin (HA), Neuraminidase (NA) and highly conserved M2 protein. Extracellular matrix protein 2 is a tetramer and forms ion channels throughout the lipid bilayer membrane. On the other hand, matrix protein M1 protein evolved from the same genomic segments and associated to the ribonucleoprotein and lipid bilayer membrane. Ribonuclear protein complex of the virus comprises PA1, PB1, PB2 NP. Small non-structural proteins are also found in unidentified position of the virion. [Adopted from (Ebrahimi and Tebianian, 2011)].

Transmembrane protein 2 (M2) is transcribed from the seventh (M) genomic segment of influenza virus. M2 protein encoding 97 amino acids is expressed from spliced mRNA of M1 mRNA (Deng et al., 2015; Ebrahimi and Tebianian, 2011; Schnell and Chou, 2008). To form a functional unit of type III protein, they form tetramer and works as ion channel of virus.

N-terminal extracellular domain of M2 protein contains (2-24) amino acids, whereas transmembrane domain comprises 25-46 amino acids and C-terminal intracellular domain is encoded by 47-97 amino acids (Ebrahimi and Tebianian, 2011). The amino acid sequence of M2 protein contains cysteine in the $17^{th}$ and $19^{th}$ position, which are well conserved and

oxidization of them helps in protein stabilization (Deng et al., 2015). pH sensitive transmembrane domain contains histidine at 37$^{th}$ and tryptophan at 41th position which function as pH sensor and gate respectively (Schnell and Chou, 2008).

Seventh segment have two parts: M1 (756 nucleotides) forms the main part of the viral capsid and M2 (291 nucleotides) membrane protein forms the ion channels (Cho et al., 2015). Both M1 and M2 protein are interrelated with each other not only in the protein form but they share their coding regions. Highly conserved M2e extracellular membrane domain of M2 protein share the first 9 amino acids with the reading frame of M1 protein. It has been revealed that different types of viruses of human, animal and avian host contain same sequence from 1-9 (gray color in Figure 2) amino acids and there might be some variability among 10-20 amino acid sequence of the M2e domain (Deng et al., 2015a). Virus types H1N1, H1N2, H3N2 those affect human, swine virus H5N1, avian virus H17N10 and bat virus type H18N11 are share consensus region (Deng et al., 2015).

They remain conjugated after translation unlit the endocytosis by the infected cells. During the endocytosis lower pH of the endosome helps to open the ion channel and balance the capsid pH. Ribonucleoprotein and Matrix protein dissociates in this condition and enter to host cell cytoplasm (Deng et al., 2015).

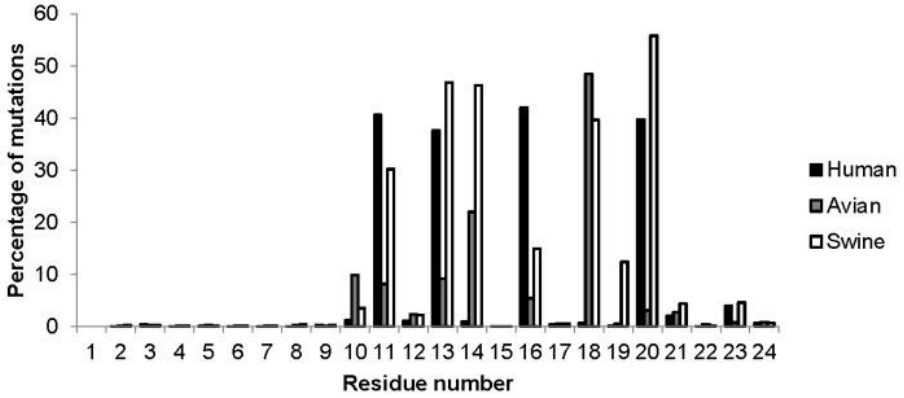


A

```
Consensus of human seasonal(H1N1) : M S L L T E V E T P I R N E W G C R C N D S S D
Consensus of human seasonal(H2N2) : - - - - - - - - - - - - - - - - - - - - - - - -
Consensus of human seasonal(H3N2) : - - - - - - - - - - - - - - - - - - - - - - - -
A/Brevig Mission/1/1918 (H1N1)    : - - - - - - - - - - T - - - - - - - - - - - - -
A/California/07/2009 (H1N1)       : - - - - - - - - - - T - S - - E - - - S - - - -
Consensus of eurasian swine (H1N1): - - - - - - - - - - T - N S E G - E - - G Y S - - - -
Consensus of eurasian swine (H3N2): - - - - - - - - - - T - N S E G - E - - - S - - - -
A/Vietnam/1203/2004 (H5N1)        : - - - - - - - - - - T - - - - E - - - S - - - -
A/Shanghai/1/2013 (H7N9)          : - - - - - - - - - - T - T G - E - N - S G - - E
A/bat/Guatemala/164/2009 (H17N10) : - - I - - - - - - T - R - - E S K - R G L N E
A/bat/Peru/033/2010 (H18N11)      : - - I - - - - - - L T - K G - E S - - S G L N E
```

B

**Figure 3.** Showing the mutation frequency in M2e domain of human, swine and avian consensus sequence. (**A)** Percentage of mutations in the consensus sequence of human, swine

and avian calculated from 14588 human,9324 avian and 3060 swine samples. (**B)** Sequence alignment of M2e virus domain revealed that, M2e is very conserved and mutation rate is also low in this consensus region among all virus types [Adopted from (Deng et al., 2015)].

Matrix protein 2 (M2) is a potential candidate for highly immunogenic vaccine based on few reasons. Firstly, vaccine against this antigen can activate complement system and cells of innate immunity. Secondly, it can bind to the infected cells and perform cell mediated cytotoxic immunity which mitigate the effectors of infected cells. Moreover, antibody binding to the antigen can prevent the release of virus particles and finally, can accelerate the phagocytosis of virus via Fc receptor pathway and helps to prevent the auto phagocytosis of infected cells (Kumar et al., 2018). Gannage et al., (2009) have reported that M2e protein is also necessary for influenza virus to prevent autophagosome and degradation. In addition to that, this virus encodes pro-apoptotic proteins which can be used as death parameter for host cell.

Amantadine (1-aminoadamantane hydrochloride) is one of the influenza virus vaccine produced targeting against the M2e membrane protein (Cao et al., 2018). This prevents the opening of the M2e ion channels and hinders the formation of M2 ion channels during the budding of new influenza virus particles (Babapoor et al., 2011). One of the problems of producing universal vaccine against M2e antigen is the lower immunogenicity of the antigen. Researchers have been trying to improve strategies to develop highly immunogenic vaccine platforms. Recombinant protein as vaccine platform is one of the used strategies to solve the problem. In some cases M2e fusion with Hepatitis B and M2e-TLR5 receptor have shown higher immunogenicity than the single M2e antigen (Ebrahimi and Tebianian, 2011).

In recent year VaxInnate Corp. (New Jersey,USA) declared M2e-flagellin fusion influenza vaccine as universal vaccine after their phase I clinical trial. After injecting two doses of 0.3 and 1 mg in young volunteers, they found 75% and >95% immunogenicity after first and second dose respectively. Moreover, two swiss companies named Cytos Biotecnology and Pevion Biotech Ltd. and two USA companies known as Dynavax technologies corp. and Merck and Co Inc. are one the way of developing M2e based universal vaccine based on M2e-AP205VLPs, M2e-Virosome, M2e-IssorNP-M2e, M2e-KLH fusion proteins respectively (Ebrahimi and Tebianian, 2011).

### 2.3 Spy-Tag-K-Tag-Spyligase

Peptide tags are the most versatile tools for detection, isolation and purification of proteins and immobilization of proteins. For decades several peptide tags have been used for this purpose and among them HA, myc, FLAG and His tags are quite common (Zakeri et al., 2012).

Formation of covalent bonds between proteins and peptides is one of the challenges for these peptide tags. Native Chemical Ligation (NCL) and Expressed protein Ligation (EPL) helps peptide bond formation but this need specific termini and limited to *In vitro* condition. Protein coupling, reconstitution is also possible in dock-and-lock system but does not work in reducing condition, one the other hand using split inteins is problematic because of its side effect. Limited stability and low bond strength between protein-peptide and temperature and pH sensitivity were the prime limitation of previously used tags (Veggiani et al., 2014).

To overcome all the limitations, researchers were searching for spontaneous isopeptide bond formation strategy development. From HK97 bacteriophage, intermolecular spontaneous isopeptide bond formation was first discovered which form chainmail by joining adjacent protein subunits (Li et al., 2014). Intramolecular isopeptide bond was found in Spy0128 subunit of pilin in *Streptococcus pyogenes* pathogen (Kang et al., 2007). This spontaneous covalent bond was shown thermal, pH and proteolytic stability which was problem in case of disulfide bonds. Recently, from CnaB2 domain of fibronectin binding protein of *S. pyogenes* another small and fast acting covalent forming pair have isolated. In the beginning CnaB2 domain was split into two fragment, 13 amino acid containing Spy-Tag and 116 amino acid containing Spy-Catcher. This pair form 50% covalent bond within 1 minutes and full reaction completed in 24 hours incubation. Spy-Tag-Spy-Catcher also work properly in different temperatures (0-60º C), pH (5-8), detergent and buffer. Spy-Tag and Spy-Catcher has become a promising tool for different applications including vaccine development (Veggiani et al., 2014). Spy-Ring cyclisation, dendrimer formation, use in resilience of enzyme and antibody-antigen ligation are some of the applications of this technology (Reddington and Howarth, 2015). Thrane et al., (2016) have reported malaria vaccine production using VARSA2CSA a malaria protein with efficient immunogenic reaction. Although Spy-Tag-Spy-Catcher provides strong bond and broad range reaction condition, the large molecular size (116 amino acid) might still be a problem in production.

To solve this limitation CnaB2 domain was split into three domains where Spy-Tag was unchanged, but Spy-Catcher was split and isolated as 10 amino acids (K-Tag) and rest of the Spy-Catcher was named as Spyligase (Figure 4). This K-Tag, Spy-Tag and Spyligase reaction optimization is our target for producing universal M2e vaccine production. Crystallography (Kang et al., 2007), NMR (Hagan et al., 2010) and quantum mechanics analysis has revealed that in conjugation reaction mechanism lysine forms covalent bond with a nucleophilic attack to asparagine with loss of H2O. Another aspartic acid/ glutamic acid residue helps to cover the

transition state of the reaction and form covalent bond between Spy-Tag and Spy-Catcher. In case of Spy-Tag, K-Tag, Spyligase, glutamic acid containing Spyligase cover the transition state and covalent bonds form between K-Tag and Spy-Tag (Kang et al., 2007).

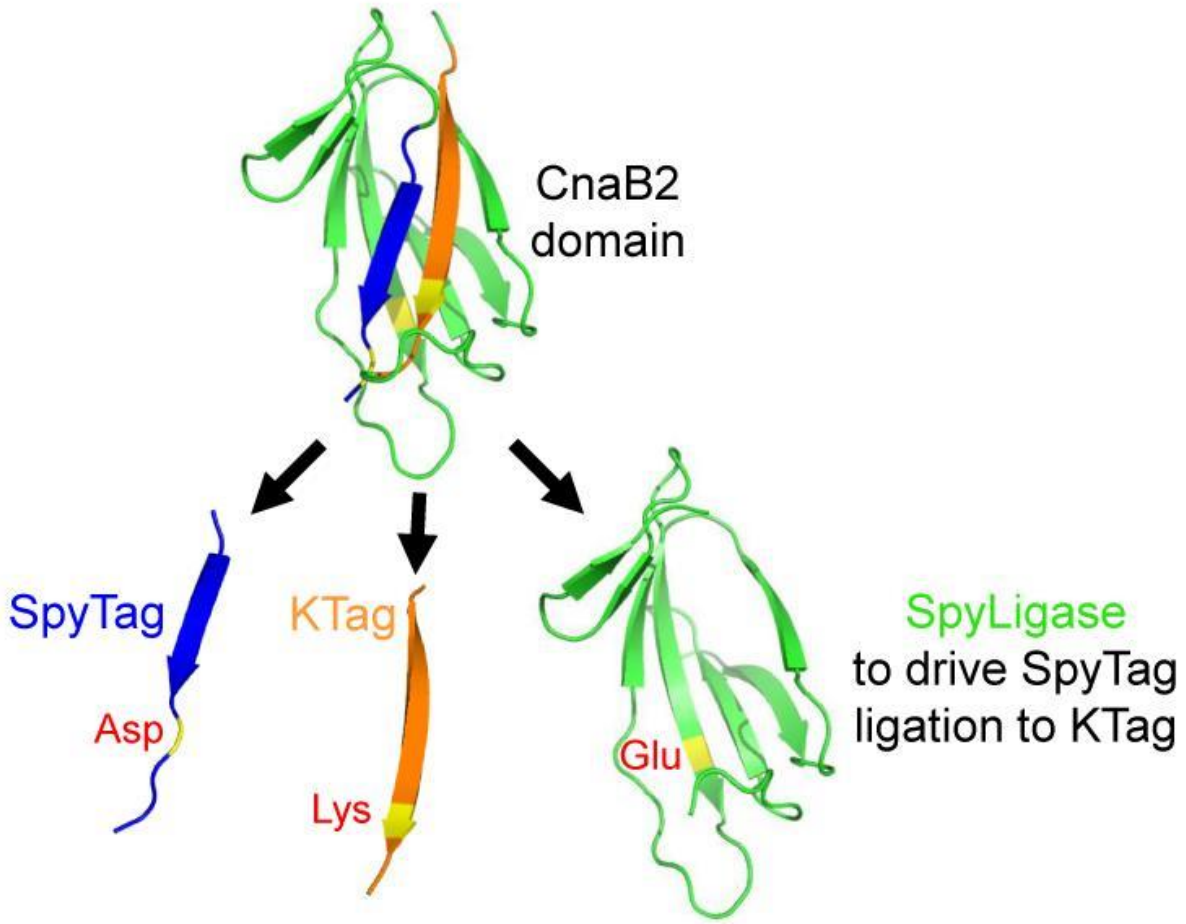


**Figure 4.** Producing isopeptide bond forming peptide tags and Spyligase. Two beta strands of CnaB2 domain have been splitted. After splitting blue colored beta strand containing aspartate named as Spy-Tag and orange colored peptide containing lysine is K-Tag and rest of the domain is Spyligase in green color. [Adopted from (Veggiani et al., 2014)].

### 2.4 Vaccines based on virus like particles

#### 2.4.1 Virus like particle overview

Vaccination is the most cost effective and successful way of preventing infectious diseases. In nineteenth century, most of the vaccines have been developed using killed or attenuated

viruses. Even though, those have been able to create strong immune responses by producing active B and T immune cells and long-lasting immunity, sometimes high production costs and safety issue have hindered their use in long run. So, researchers have been searching for alternative vaccine production methods which would be cost effective and safe (Mohsen et al., 2017).Virus like particles are nano-scale protein components, similar in morphology and structure to native virus particles (Rodríguez-Limas et al., 2013). It is organized macromolecular empty shell form by the assembly of viral structural proteins (capsid) (Liu et al., 2014). Though they are very similar in their morphology but do not contain any genetic material and noninfectious (Santi et al., 2006). VLPs can be produced by genetic engineering and expressing the viral structural proteins in different host cells of mammalian, insect, plant and yeast or bacteria (Santi et al., 2006).

In the past three decades virus like particles (VLPs) have become the most potential tool in the field of vaccine development (Zeltins, 2013). VLPs constitute versatile tools in vaccine development due to their favorable immunological characteristics such as their size, repetitive surface geometry, ability to induce both innate and adaptive immune responses as well as being safe templates with promising economics (Mohsen et al., 2017)**.** VLPs are multi-protein supra-molecular structures and carry many characteristics of viruses that can be harnessed in vaccine development strategies (Mohsen et al., 2017). They are very small (20-100 nm) in diameter which permit entry and exit in various lymph nodes, lymphatic vessels throughout the body and facilitate optimal uptake by antigen presenting cells (Frietze et al., 2016).

VLPs have lots of resemblances with the inactivated virus particles. Prior to use and development of the VLPs, inactivated viruses were the most efficient vaccines (Bright et al., 2007). Including polio, hepatitis A, Influenza, Japanese Encephalitis and Rabies several vaccines have been approved by FDA which were produced using inactivated viruses (Bright et al., 2007). Effective antigen is the target of vaccines, sometimes antigens alone do not provide good response, but some adjuvant formulation might be given for better responses. Bacterial toxins, cytokines, polymeric particles, emulsions, pathogenic receptors, liposomes and aluminum salts are the most commonly used adjuvants in VLP based vaccines (Cimica and Galarza, 2017; Debbink, 2015). Nowadays there are several commercially available VLP based vaccines e.g. Hepatitis B vaccine and human papilloma virus vaccines. Mostly they have been produced by expressing recombinant non-enveloped structural proteins in mammalian, insect, yeast, plant or bacterial cells (Quan et al., 2016).

Vaccines based on VLPs are more immunogenic than the protein subunit vaccines (Frietze et al., 2016). VLP platform allows to present antigens in high density and repetitive manner which helps to attract the crosslinking of B cell receptors and produce strong vaccines. Cross linking of the antigens helps to present the VLPs to the different types of cells like CD4 and DC8. Moreover, to MHC I and MHC II molecules which increases the response against antigens (Quan et al., 2016).

VLPs exhibit repetitive surface antigens on their icosahedral or helical structures (Frietze et al., 2016). There are many different hosts for producing the virus like particles. Among them human (Jones et al., 2015), insect, plant (Santi et al., 2006), yeast (Wetzel et al., 2018) and bacterial (Huo et al., 2018) production systems are the most popular. However, more than 30% VLPs have been produced using the bacterial production system under strong promoter in plasmid construct and codon optimization have been done to optimize the production (Mohsen et al., 2017).

### 2.4.2 Examples of VLP vaccines and technologies

From last three decades, VLP-based vaccine research has been very prominent due to its effective and qualitative nature. Yang et al., (2017) have reported a vaccine production against Zika (ZIKV) virus. They have used Hepatitis B core antigen for devising VLP which display ZIKV E Zika virus protein domain III (zDIII). This HBcAg-Zdiii VLP can be easily produced in *Nicotinia benthamiana* plant cells and are highly immunogenic. This newly invented vaccine elicited potent cellular and humoral responses in mice trial against several Zika virus strains. Moreover, it has overcome cross-inducing antibody limitation, including sensitizing people to subsequent dengue virus (DENV) infection. Improved safety, lower cost and equivalent effectiveness makes dengue VLP popular over current alternatives (Yang et al., 2017).

Last year, a group of scientists have successfully expressed VLPs in yeast production system. They have fused eight different antigens of different animal Hepatitis virus to the VLP, where antigen size was also different (Wetzel et al., 2018).

Several VLP-based vaccines are now available against different chronic and fatal diseases including cancer and HIV (Shouval et al., 2015). After first development of Hepatitis virus based VLP-vaccine (HBsAg-VLP) in 1980, many limitations such as safety and tolerability have been overcomed (Shouval et al., 2015). Blumberg developed second generation hepatitis B (HVB) vaccine expressing SHBs (structural protein of hepatitis B) protein of HVB virus in the *S. cerevisiae* and proved the effectiveness of VLPs. Currently, one of the third generation HVB vaccine Sci-B-Vac$^{TM}$ has been approved to use in 14 east Asian countries including Israel.

Sci-B-Vac™ Vaccine clinical trial data, in chronic patient of hepatitis of Vietnam showed 50 % suppression, incorporation of the lamivudine oral adjuvant (Shouval et al., 2015).

Malaria is still a threatening disease in the whole world, until last year there was no commercial vaccine against malaria. Mosquirix™ is a recent and only reported and certified malaria vaccine using virus like particle targeting pre-erythrocytic stage (Moorthy and Ballou, 2009). In the N-terminus of the HBsAg-VLP, malaria antigen consisting central repeat of B and C-terminus repeat of T-epitope has fused in addition to MLP and QS-1 adjuvent (Moorthy and Ballou, 2009). The strategy of using adjuvants are not new, many adjuvants have been used for getting proper antigenic response and activating the adaptive immunity through stimulating the innate immune response (Moorthy and Ballou, 2009). 3-O-desacyl-4'-monophosphoryl lipid A (MPL) and saponin are two frequently used immune-stimulants in the candidate vaccines based on VLPs (Ding et al., 2018). The adjuvant system AS04 contains the MPL and aluminum salts whether, AS01 and AS02 contains the MPL and QS-21, are liposome and emulsion based formulations respectively (Van Mechelen, 2011). Cao et al., (2018) have reported a successful development of Virus like particle-based cancer therapeutics for targeted photodynamic therapy. In this protocol targeted photosensitizers absorb light and produces the oxygen radical to kill the cancer cells (Brady et al., 2017).

Human papilloma virus (HPV) is the most common sexually transmitted large virus group causing a greatest risk of cervical cancer (Burd, 2003). This virus group comprises more than 150 types HPV viruses(Centre for disease control and prevention, 2019). Cervarix, Gardasil and Gardasil9 are the three FDA approved vaccines based on HPV virus like particle (De Vincenzo et al., 2014). In the year of 2006, first VLP-based vaccine against HPV type 6, 11, 16 and 18 was approved by FDA (De Vincenzo et al., 2014). In the following year vaccine named cervarix, targeting only HPV 16 and 18 was approved. In 2014, Gardasil9 has been approved and it was more immunogenic and efficient against broader range of viruses than before (De Vincenzo et al., 2014). HPV type 45, 52 and 58 which are responsible for 20% of current cervical cancer were included in the vaccine Gardasil9 (Harper et al., 2017). Recombinant L1 capsid protein of HPV virus have been used to produce HPV VLP and aluminum hydroxyphosphate neutral salts have used as adjuvant (De Vincenzo et al., 2014).

Rotaviruses are causative agents of diarrhea and are health threats all over the world (Lamrani et al., 2017). Though Rotashield, Rotateq and Rotarix are three attenuated Rotavirus vaccines, they are not sufficient for complete prevention of the virus. Currently, VP2 and VP6 protein

have been used to produce single and double layer VLPs to fight against this virus, which have shown higher immunity than the previously used vaccines (Li et al., 2014).

Akahata et al., (2010) have reported successful VLP based vaccine construction against epidemic causing Chikungunya virus (CHIKV). Chikungunya virus is a mosquito borne alpha virus of Togaviridae family, isolated first in Tanzania. Infection of this virus can be characterized by rash, high fever and it causes severe arthritis which lasted 1-2 year (Akahata et al., 2010).This vaccine construct was found to produce a response in Monkey immunization experiment preventing CHIKV attack by inducing humoral immunity.

Drug delivery in cancer treatment via His-tagged Virus like Nano-structure particles has been done successfully by (Biabanikhankahdani et al., 2017). The strategy they have applied is that, targeted therapeutics Doxorubicin (DOX), have been conjugated to virus like particles using nitrilotriacetic acid (NTA). The His-tagged VLPs joined via non-covalent bond with DOX-NTA and cross-linked with folic acid (FA) which is released in the ovarian cancer cells through folate receptors (FR).

### 2.4.3 Function and application of VLP

Willis et al., (2008) have concluded that Virus like particles have the potential application to produce soluble probes for membrane protein interaction by incorporating conformational-complex membrane protein. To solve the problem of studying reactivity of integral membrane proteins and their kinetic differences of reaction, they have analyzed this molecular technique of VLP-based lipoparticles. They have used the G-protein coupled receptor membrane protein to quantify the kinetic difference of reactivity of market available antibody against chemokine receptor CCR5. Recent investigation of vaccines based on VLPs has proved their efficiency and safety in different clinical trials. Protein engineering application made possible to get enveloped proteins of right confirmation and higher immunogenicity (Quan et al., 2016).

Most of the current influenza vaccines targeted on a strain specific transmembrane protein is not sufficient to control the pandemics. Virus like particles can be used to produce universal vaccine to deteriorate the outbreaks. It is possible to use conserved antigens as a surface protein of the VLP with a perfect conformation, in addition to an adjuvant which produces very immunogenic vaccines (Kang et al., 2012). VLPs can be used not only for vaccine productions but also in drug delivery, incorporating nucleic acids and small molecules (Santi et al., 2006).

### 2.4.4 Norovirus and VLP

Noroviruses are one of the prime gastroenteritis epidemics causing viruses of Caliciviridae family (Robilotti-Cairlet et al., 2015). These plus (+) stranded highly infectious RNA viruses

are responsible for almost 95% viral outbreaks which spread through food contamination and personal contact (Karst, 2010). Noroviruses are frequently divided into five genogroups including GI, GII, GIII, GIV and GV. Among them GI, GII and GIV are human viruses, GIII is bovine and GV is murine Noro virus (Karst, 2010). Non-enveloped icosahedral Noroviruses are small in diameter (38-40 nm) (Karst, 2010), major capsid protein (VP1) encoded from ORF2. This capsid includes conserved internal shell (S) and variable protruding (P) domain. P domain is further subdivided into two domains (P1 and P2). Production of VP1 domain (independently of other viral components) results in the self-assembly of the VLPs. A fully functional Norovirus contains 180 copies of VP1 protein in the capsid (Karst, 2010). Because of its small size and high VP1 protein copy number, this VLP is experimentally used as vaccine platform. However, it is still necessary to optimize the production rate, post translational modification and proper purification method which is hindering its application (Jones et al., 2015). One possible production system was human B cell in case of Sydney human norovirus (HuNoV) strain but still need optimization (Jones et al., 2015). In a report of Huo et al, (2018) they have claimed that, *E. coli* BL21 could produce enough VP1 protein by using pCold III and pCold IV vectors.

White et al., (1997) have claimed a successful production of Norwalk virus and VP1 protein in Sf-9 insect cells. After purification using CsCl and sucrose gradient it gave a good immune response in the animal trial. However, this process was not cost-effective, moreover, it was time consuming. In recent years, Koho et al. (2015) successfully expressed this Noro VLP in insect cells and purified using ion exchange chromatography, which is very fast and cost-effective method. Later, decoration of His-Tagged Noro VLPs enabled its purification by using affinity chromatography (Camper and Viola, 2009). There is no commercially available Noro-VLP based vaccine available yet (Lucero et al., 2018).

# 3 Aims of the thesis

The aim of this thesis was to test the ability of Spyligase protein in conjugating Spy-Tagged and K-Tagged vaccine components together. However, the first aim was to produce and purify a Spy-Tagged norovirus-like particle (Spy Noro VLP) as a vaccine platform and Spyligase protein, which is an enzyme conjugating Spy-Tag and K-Tag together. Before performing the conjugation reaction, K-Tagged influenza-antigen M2e was ordered as synthetic peptide. Wild Type Norovirus-like particle (WT Noro VLP) was produced and purified as control antigen for the conjugation reaction.

Specific aims of the study were

1. To produce and purify
    a. Spy-Tagged Noro VLP,
    b. Spyligase protein and
    c. WT Noro VLP
2. To test the ability of Spyligase in conjugating Spy-Tagged Noro VLP with K-Tagged M2e antigens.

From last three decades scientist have been utilizing Virus-like particles intensively for vaccine production. Different VLP platforms have been replacing the live attenuated and inactivated virus vaccines as well as peptide antigens as vaccine candidates. Noro VLPs are a perfect choice for VLP based vaccine production due to its easy production and purification. In a previous study by (Koho et al., 2015) a successful production of His-Tagged Noro VLP has been shown, which have been used for immobilizing streptavidin-biotin Tris-NTA conjugates and fluorescent dye molecules. Recently, Spy-Tag-Spy-Catcher have been used intensively for protein conjugation but large molecular size of Spy-Catcher which may cause immune reaction is still a limiting factor for vaccine production (Reddington and Howarth, 2015). In this study, spliced parts of CnaB2 fibronectin binding domain (Spy-Tag and K-Tag) were conjugated in the reaction mixture catalyzed by Spyligase to form influenza M2e antigen decorated Noro VLPs.

# 4 Materials and methods

## 4.1 Insect cell culture

In this study insect cells were used for producing Spy Noro VLP and WT Noro VLP. Sf-9 cells (*spodoptera-frugiperda*) were used for baculovirus (BV) amplification and Hi-5 cells (*Trichoplusia ni*) and TNI-FNL-Hi-5 were used in the production of VLPs. The cells were maintained in 100 ml suspension cultures in plastic cell culture bottles, so that, culture bottles at least contain five times free space for sufficient gas exchange. Cells were cultured at 27° C in 225 rpm constant shaking. Lonza insect- XPRESS protein free insect cell culture medium containing L-glutamine without antibiotics was used. In the culture, 10 U/ml heparin was used in case of Hi-5 and TNI-FNL-Hi-5 cells to avoid cell clumping. Cells were split thrice a week to keep them in continuous log phase. One day before starting VLP productions the cells were split and only >95% viable cells were used for production. CountessTM bench top automated cell counter (Invitrogen CA, USA) was used for estimating cell numbers and trypan blue was used for staining the dead cells. The cells were regularly observed with a microscope.

## 4.2 Baculovirus stock production

### 4.2.1 Production of P1 virus stock

Baculovirus stock production (P1) was started with the transfection of the Sf-9 cells with the Spy Noro VLP Bacmid prepared previously (Bac-to-bac baculovirus expression system, Invitrogen by life technologies). The cells were transfected with 1 µg bacmid DNA using baculoFECTIN II reagent following the baculoFECTIN II user guide (https://oetltd.com/wp; 20.01.19). After counting the cells, 2 ml cell suspension containing 0.5 x $10^6$ /ml was plated in a 6 well plate and let adhere for 60 minutes in order to form sub-confluent monolayer of cells. 100 µl cell culture medium, 1 µg bacmid DNA and 1.2 µl BaculoFECTIN II reagent (Oxford expression technologies, Oxford, UK) was added into a sterile disposable 1.5 ml tube, mixed well and incubated for 20 minutes to form the nanoparticle DNA complex. After the cell monolayer formation, 1 ml cell culture media was removed from each well carefully so that, it does not disturb the cells and 0.1 ml BaculoFECTIN II/DNA mixture were added dropwise on the cells. Then the plate was placed in a sandwich box containing moistened paper and incubated at 27°C over night. Then 1 ml medium per well was added and the cells were incubated for another 4 days. Five days post infection (dpi) the cells and the supernatant were collected by centrifugation 200g for 5 minutes in a table top centrifuge and the supernatant was filtered using 0.20 µm filter (GE Healthcare Life Sciences, USA). Following the separation,

supernatant and cells were stored in 4°C and-20°C respectively. This supernatant was P1 BV stock which was used for producing P2 BV stock.

### 4.2.2 Production of P2 and P3 virus stocks:

Sf-9 cells were prepared for infection to produce the P2 stock. 200 ml cells containing 2 x $10^6$ /ml was cultured in a 2 L bottle and infected with P1 stock in 1:200 volumetric ratio. 6 dpi P2 BV stock was collected by centrifugation in 2500 g for 10 minutes at room temperature (RT). Before centrifugation 1% FBS was added in the culture to enhance BV stability. The supernatant was filtered consecutively through 0.45 and 0.20 µm filters (GE Healthcare Life Sciences, USA). P3 BV stock was prepared by infecting another 200 ml of cells (2 x $10^6$ cells/ml) with P2 stock.

WT Noro VLP P2 stock produced previously in the laboratory was used to infect 200 ml Sf-9 in a 1:200 volumetric ratio. Cell viability was >95% by the time of infection. Transfected cells and supernatant were collected 5 dpi following the same protocol used for the Spy Noro VLP stocks.

### 4.2.3 Optimization of protein production

For producing the highest amount of VLPs, small scale test productions were done for Spy Noro VLP and WT Noro VLP using Hi-5 and TNI-FNL-Hi-5 cells. In different batches of test production, P2 and P3 virus stocks of Spy Noro VLP and only P3 stock of WT Noro VLP were used both in Hi-5 and TNI-FNL-Hi-5 cells. Every test production volume was 50 ml and cell concentration were 2 x $10^6$ / ml and viability were more than 95%. P2 and P3 BV stocks of both VLPs were added in different volumetric ratio in both cell lines. All test productions were harvested 6 dpi (applying the same technique as described before in virus stock production).

## 4.3 Large scale Noro VLP production

In all production batches, 1:50 virus dilution was used for Spy Noro and WT Noro VLP protein. Cells were split the previous day of infection to keep them in early log phage. Culture volume was 10 x 100 ml and 2 L Erlenmeyer plastic screw cap culture bottle was used. Cultures were harvested 6 dpi. For harvesting 1-liter culture, 20 g sartoclear dynamics lab filter aid (Sartorius Filter aid, Germany) was added and mixed well and filtered through 0.20 µm Nalgene Rapid Flow 500 ml bottle Top filter (Thermo Fisher Scientific, Wilmington, USA) using vacuum pump. Cell pellet and supernatant sample of Spy Noro and WT Noro VLP were taken and analyzed in Stain-free SDS-PAGE gel electrophoresis (*Detailed mechanism in chapter 4.10.1*).

Protein bands of the expected size were observed in the SDS-PAGE gel where band intensity was used to determine the production level and BV dilution for optimal production level for both proteins.

### 4.4 Purification of Noro VLP

#### 4.4.1 Tangential flow filtration

Noro VLPs were purified by following multi-step protein purification process. Hi-5 culture supernatant containing the produced VLPs was cleared as described above (section 4.3). The culture supernatant was concentrated with tangential flow filtration using AKTA Flux s instrument (*Detailed method at 4.10.4*), and 750 MWCO hollow fiber (#UFP-750-E-3X2MA, GE Healthcare). After washing the system and the hollow fiber with Milli Q water, sample was applied in the tank. The transmembrane pressure was around 0.3 MPa during the sample application and wash and elution fraction tank level settled at 100 g. Concentrated 186 g (100 g sample + 86 g binding buffer) Noro VLPs were collected in a clean bottle. Small sample from both permeate and concentrated Noro VLPs were collected for SDS-PAGE gel analysis. Here, 50 mM phosphate buffer pH 7.0 was used as binding buffer.

#### 4.4.2 Ultracentrifugation

Noro VLP was finally concentrated with ultracentrifugation using 30% sucrose cushion pelleting in phosphate-buffered saline (PBS). Optima XPN-100 ultracentrifuge (Beckman) with Rotor SW32Ti and 38.5 ml ultra clear tubes (#344058) were used. Sucrose cushion gradient was made by pipetting 6 ml 30% sucrose in 38.5 ml tube and 31 ml of TFF concentrated Noro VLP sample on the top of the sucrose. VLPs were pelleted with ultracentrifugation for 16 h, 32000 rpm at 4 ˚C. After ultracentrifugation, supernatant was fractionated into four five ml and rest of them in 1 ml fractions and carefully removed the last drops of the supernatant using cellulose paper. The pellets were dissolved in 1 ml PBS by magnetic stirring 4 hours at 4˚C. Another 500 µl PBS buffer was added and transferred to Eppendorf tube and centrifuged 5 minutes at 13000 g at 4 ˚C. Small sample of the starting material, fractions after the ultracentrifugation, pellet and supernatant were collected and analyzed in SDS-PAGE gel.

#### 4.4.3 Anion exchange chromatography

Anion exchange chromatography was used as the final purification step for the VLPs *(Detailed mechanism in chapter 4.10.5)*. HiTrap Q FF 5 ml or 50 ml (GE HealthCare, Chicago, USA)

column was connected to the AKTA Start chromatography instrument. A buffer containing 50 mM $NaH_2PO_4$ (pH 7.0) was used as the running buffer, and buffer containing additionally 1 M NaCl was used as the elution buffer. Prior to sample application column was prepared following the column manual and the concentrated VLP was diluted with 50 mM phosphate buffer until the conductivity reached 3.5 $mS/cm^2$. After sample loading, the column was washed to remove unbound protein and column-bound VLPs were eluted using 100% gradient.

### 4.5 Production of Spyligase

#### 4.5.1 Plasmid recovery

A Bacterial stab containing DH5α *(E. coli)* transformed bacteria, were received from Addgene company (Addgene, Watertown, Massachusetts, USA). Transformed bacteria contain N-terminally His-Tagged Spyligase in pDEST14 plasmid. Bacteria were streaked onto an ampicillin-glucose-LB plate and incubated overnight. In the following day, selected single colonies were inoculated in four tubes of 5 ml ampicillin-glucose-LB medium. Tubes were incubated at 37°C in 228 rpm shaking. After 6 hours, 2 ml of bacterial liquid culture was added to 200 ml of ampicillin-glucose-LB medium. In next day, the $OD_{600}$ was 0.764 in 1:20 dilution. The culture was centrifuged 10 minutes at 4300 rpm at 4°C and the bacterial cell pellet was resuspended in 50 ml PBS buffer and plasmid DNA was isolated by using NulceoBond Xtra Midi plus EF kit by Macherey-Nagel *(Detailed in chapter 4.10.3).* Concentration of the plasmid DNA was determined by measuring 280 nm absorbance with NanoDrop spectrophotometer . The plasmid DNA was then aliquoted and stored in the freezer (-80 °C).

#### 4.5.2 Chemical transformation of plasmid into competent bacteria

1 µl (84.3 ng/µl) pDEST14-Spyligase plasmid was transformed into, BL21 Star DE3 bacterial strain using the heat shock method (30 s, +42°C) and transformed bacteria were selected based on their growth on ampicillin containing LB plates. 100 µl and 20 µl of the transformed bacterial cells were spread evenly on amp-gluc-LB plates and let grow overnight (to obtain single colonies).

#### 4.5.3 Spyligase culture condition optimization

Successful transformation allows bacteria to grow into ampicillin-glucose-LB plate and in the plate single colonies were identified. Single colonies were inoculated into 5 ml LB, supplemented with 0.1 mg/ml ampicillin and 0.45 mg/ml glucose and incubated overnight at 37°C, in 160 rpm constant shaking. Three different temperatures were tested to find out which

temperature produces the highest amount of Spyligase. Before inoculating, seed culture was centrifuged at 4000 g for 10 minutes and the pellets were resuspended in 5 ml of culture medium. After that, 3x200ml ampicillin-glucose-LB medium were prepared and 2 ml of resuspended seed culture was inoculated in each flask. Antifoaming (10 µl structrol) agent was used to reduce the foaming. When $OD_{(600)}$ was ~0.4; 200 µl (1mM) IPTG protein production induction agent was added and incubated overnight at 18°C, 25°C or 37°C in 228 rpm constant shaking. Small scale Nickel-NTI-resin protein purification was done by using EasyLyze kit. Pellet, supernatant and resin sample were collected and run into the SDS-PAGE gel.

### 4.5.4 Spyligase purification

1 L of bacterial culture containing Spyligase was centrifuged at 4300 g for 10 minutes and the supernatant was removed and resuspended with binding buffer (50 mM NaHPO4, 500 mM NaCl and 10 mM imidazole). Bacterial cells were lysed using Emulsiflex-C3 (Avestin, Ottawa, Canada) homogenizer instrument, sample was passed twice through the valve at 60-100 bar. Then the lysates were centrifuged 10 minutes at 20000 g in 4°C (Thermo scientific LyNX 4000 centrifuge) to separate the pellet and the supernatant. Pellet and supernatant samples were collected for SDS-PAGE for further analysis. In the final step of Spyligase purification Immobilized Metal Affinity Chromatography (IMAC) was used. To purify histidine tagged Spyligase, HisTrap FF Crude 5 ml column (GE Healthcare, Chicago, USA) was used. Before sample application column was connected to the AKTA START (GE Healthcare, Chicago, USA) instrument and prepared by thoroughly washing with water and equilibrated with the mobile phase buffer. After column equilibration the sample was applied to the column and washed with binding buffer to remove the unbound proteins from to the column. Then column bound proteins were eluted using elution buffer (50 mM NaHPO4, 500 mM NaCl, 250 mM imidazole, pH 7.5) in 5 ml fractions. Small load, wash, Flow through and elution fractions samples were collected for analysis in SDS-PAGE gel.

### 4.6 Endotoxin removal from the protein

According to endotoxin measurement assay (chromogenic LAL assay) purified Spyligase and Spy Noro VLP contained high levels of endotoxins. For removal of endotoxins from the Spyligase protein, the protein was bound to nickel sepharose column (HisTrap Q FF Crude pre-made 5 ml column (GE Healthcare, Chicago, USA) ) and washed with 0.1% Triton X114 (0.1% triton X 114 was added into the 50 mM phosphate buffer). Column was connected to the AKTA Start column chromatography instrument (GE Healthcare, Chicago, USA). After sample

loading into the column it was washed with binding buffer containing 0.1% Triton X114 binding buffer Spyligase protein was eluted from the column using 250 mM imidazole and fractionated in 5 ml fractions. After elution fraction pooling together, dialysis was done, and concentration was measured by BCA analysis method. Prior to use LAL assay protein sample was diluted 10 and 20 folds and 10 µl diluted sample was mixed with limulus amebocyte lysates and chromatogenic substrate. When incubation was completed, absorbance was measured using 405 nm light. A standard curve was created from the absorbance data and calculated endotoxin level.

### 4.7 Dialysis of the proteins

Dialysis of IMAC purified Spyligase was performed using commercial Slide-A-Lyzer(R) dialysis cassette (Thermo Scientific, Rockford, USA). Observing chromatogram peaks, protein containing elution fractions from IMAC purification were pooled and injected into hydrated dialysis cassette (using a syringe and needle) to remove imidazole gradually from the sample. The cassette was sunk into 2 L PBS including 1% EDTA and 100 ml imidazole dialysis buffer (1x) in continuous stirring using magnetic rods. Imidazole amount in the PBS buffer was reduced gradually and the buffer was changed three times after every two hours and put over night in PBS at 4ºC. When the dialysis was complete, the sample was removed from the cassette into a clean tube and the concentration of the sample was determined with BCA analysis.

### 4.8 Dynamic light scattering analysis

Purified protein sample was put into the plastic cuvette and set to the Zetasizer Nano ZS (Malvern Instruments, Worcestershire, UK). The viscosity of the sample buffer was used as the viscosity of the sample at 25°C. PBS was the sample buffer for dialysed samples of Spy Noro and WT Noro VLPs. On the other hand, 50 mM phosphate including 0.5 M NaCl was used as sample buffer for elution fraction samples of Spy Noro VLP. In case of all samples of Spy Noro VLP and WT Noro VLP 100 µl was loaded into the cuvette. (*Detailed in chapter 4.10.6*).

### 4.9 Conjugation reaction of Spy Noro VLP and K-Tagged antigen

Following the production and purification of the Spyligase and Spy Noro VLP and dissolving K-Tagged-M2e synthetic peptide, conjugation reaction was performed. Both Spyligase and Spy Noro VLP were in PBS buffer, but K-Tagged-M2e antigen was dissolved into PCT buffer. Spy Noro VLP, Spyligase and K-Tagged-M2e antigen were mixed in 1:3:20 molar ratio. The reaction mixture was incubated at 4°C for 24 hours, analysed in SDS-PAGE gel and western

blotting (*Detailed in chapter 4.10.2* ) using the M2e specific mouse monoclonal antibody. IRdye containing secondary antibody was used against primary antibody to measure the intensity of primary antibody and imaged in Odyssey CLx (LI-COR Biotechnology, Lincoln, USA) instrument. IRdye of secondary antibody is sensitive at 800 nm light channel and marker at 700 nm light channel in odyssey instrument.

## 4.10 Detailed methods and protocols

### 4.10.1 SDS-PAGE

Sodium Dodecyl Sulphate Polyacrylamide Gel Electrophoresis (SDS-PAGE) is one of the vital techniques for identification of proteins and nucleic acids of a sample. The SDS (sodium dodecyl sulphate) is highly negatively charged and it neutralises the protein in the gel (Al-Tubuly, 2000). This is the cause of smooth running of protein and peptides and nucleic acids in gel and bigger protein run more slowly than the smaller ones. Boiling of the protein together with the sample buffer helps to denature the protein. Instantly, SDS occupy the positive charge of protein and help to linearize the protein.

In basics, polyacrylamide gels are formed by the polymerisation of crosslinked acrylamide, bis-acrylamide in presence of one catalyst and initiator. Ammonium persulfate (APS) is a source of persulphate ions (S2O8-) used as solidifying initiator and free radical source. TEMED (N,N,N',N'-tetramethylethylenediamine) catalyse the reaction by stabilising above mentioned free radicals.

(https://www.thermofisher.com/content/dam/LifeTech/global/Forms/PDF/protein-gel-electrophoresis-technical-handbook. pdf).

In protein and protein dynamics SDS-PAGE technique is highly used because of its accuracy, easiness and cost-effectiveness. In our study, SDS-PAGE was used for identification of the Spyligase, Spy Noro VLP, WT Noro VLP proteins and analyzing protein conjugation. The samples were mixed with sample buffer including mercaptoethanol and heated for 10 minutes at 100°C. Self-made 12% polyacrylamide gels were prepared by using the TGX stain free Fast-Cast acrylamide Kit (BIO-RAD, Hercules, California, USA). We have also used any KD PROTEIN Mini TGX stain free precast gels and any KD CRITERION TGX stain free protein gels. For referencing the protein bands, unstained protein ladder was used with protein sample in the gel.

Stain free gel technology uses the ability of the aromatic amino acid tryptophan to react with the trihalo compound during their exposure to UV radiation. The compound emitted fluorescence from the one tryptophan residue can detect 20-50 ng of protein in the gel (https://www.bio-rad.com/en-fi/applications-technologies/stain-free-imaging-technology?ID=NZ0G1815, 04.01.19). Imaging of stain free gel was done by using ChemiDoc XRS+ (BIO-RAD, Hercules, California, USA).

### 4.10.2 Western blotting

Western blotting was used to specifically detect the antigens with antibodies. After completing SDS-PAGE the proteins were transferred (blotted) onto nitrocellulose membrane by using Trans Blot Turbo blotting system (Bio-Rad, California, UDA). The proper transfer of the proteins was confirmed by imaging with Odyssey instrument.

Ponceau S (Sigma-Aldrich, St Louis, USA) stain was used to detect PageRuler unstained protein marker from the nitrocellulose membrane. As it is negatively charged, it easily and effectively binds to the positive amino group of the protein and they also form non-covalent bonds in the nonpolar protein region (Al-Tubuly, 2000). Visualised marker bands were marked with a Western blot marker pen (LI-COR, Biotechnology, Lincoln, USA). Blocking buffer (5% BSA-TBS-Tween-80) was used to block the other binding area of the nitrocellulose membrane. Primary antibody was added in a ratio of 1:3000 and incubated for 1 hour. After washing the membrane x 3 with TBS-0.05% Tween20, secondary antibody was added (1:5000) and incubated for 1 hour. Finally, nitrocellulose membrane was washed x 3 with TBS-0.05% Tween20 and soaked into TBS before Odyssey analysis to remove tween20 before imaging. The stained blot was scanned with Odyssey instrument using both channels of 700 nm and 800 nm light bundles. Membrane was imaged with the Odyssey CLx instrument (LI-COR, Biotechnology, Lincoln, USA).

### 4.10.3 plasmid recovery protocol

DH5 Alpha *E. coli* bacterial strain is developed by Douglas Hanahan (https://cgsc2.biology.yale.edu/index.php, 06.01.19). This bacterial strain is mutated for better transformation and retaining high genetic materials inside the bacteria. As a gram-negative bacterial strain, it is easy to lysate the cell wall with lysis buffer. Bacterial cells are recommended to grow at 37ºC in the LB medium with constant shaking in over 200 rpm. Selection pressure is important for continuous cell division and plasmid manipulation. Proper culture condition also requires 4-5 times more space of the culture flask for enough gas

exchange. In case of Midi plus plasmid isolation culture volume changes on the basis of $OD_{(600)}$ is sometimes required to dilute first for the proper measurement of the cell density into1:20 (https://www.mnnet.com, 06.01.19). Yield of the plasmid DNA also depends highly on the size of DNA and origin of replication. Chloramphenicol can be used to increase the yield in case of low yield plasmid. Bacterial pellet resuspended into buffer containing Tris, EDTA, glucose and RNase A. Divalent cations are necessary for DNase activity which chelates by EDTA and prevents the plasmid lysis. RNase A degrades cellular RNA, whereas glucose maintain the osmotic pressure and prevent burst out of cells (https://bitesizebio.com ,06.01.19). The lysis buffer contains sodium hydroxide and SDS detergent. SDS solubilize the cell membrane and NaOH breaks the cell wall and most of the protein. Moreover, NaOH helps to break the hydrogen bonds between the DNA and converts the double helix protein molecule into single helix. Gentle mixing of resuspension buffer and lysis buffer is very important to work well but shaking or centrifugation may cause damage of the plasmid DNA. Neutralizing buffer contains potassium acetate which make a condition of reannealing of the single stranded DNA into double stranded DNA (https://bitesizebio.com, 06.01.19). Comparative small DNA fragments of plasmid DNA reanneal quickly, and genomic DNA are not able to do so, but if it breaks into small pieces because of rapid shaking it may cause impurities of our plasmid DNA sample. Three steps washing with three different buffers is very important to remove the high salt concentration and removal of the endotoxins and separating the plasmid. In the final step of the plasmid isolation the elution buffer of higher salt concentration neutralizes the resin binding the plasmid DNA and elute from the column. Finally, the eluted plasmids precipitate by adding small amount of isopropanol in the solution separates by following concentrating protocol. (https://www.mnnet.com, 06. 01.19).

### 4.10.4 Tangential flow filtration

In this technique the sample solution is passed tangentially along the pressurized filter surface. Depending on the necessity, different types of membranes can be used for different purposes. Micro-filter Membrane with 0.1-10 µm pore size is generally used in sterilization, clarification and removal of small particles. Ultrafiltration membrane with pore size 0.1-0.001 µm can be used for concentrating, desalting and buffer change of the sample. Sample applied to tangentially along the membrane is named as feed, passed solutions across the membrane is known as permeate and retained solution to the tank is retentate. When sample solution is loaded to the tank and passed through the membrane a constant pressure is applied which help to remove the small particles and start concentrating the sample (Figure 5). It is advisable to

use 3-6 times lower molecular weight cut off membrane than the protein or other sample molecular weight. Pressure needs to be individually determined to each target sample to get good yield of the target sample. Concentrating and diafiltrating are two different parts of TFF. After concentrating, diafiltrating (buffer changing) can be done. In this continuous process buffer of interest is added to the reservoir in a constant pace so that reservoir sample volume remains constant. Even small molecules and salt and ions can be removed by using tangential flow filtration. (https://laboratory.pall.com/content, 08.01.19).

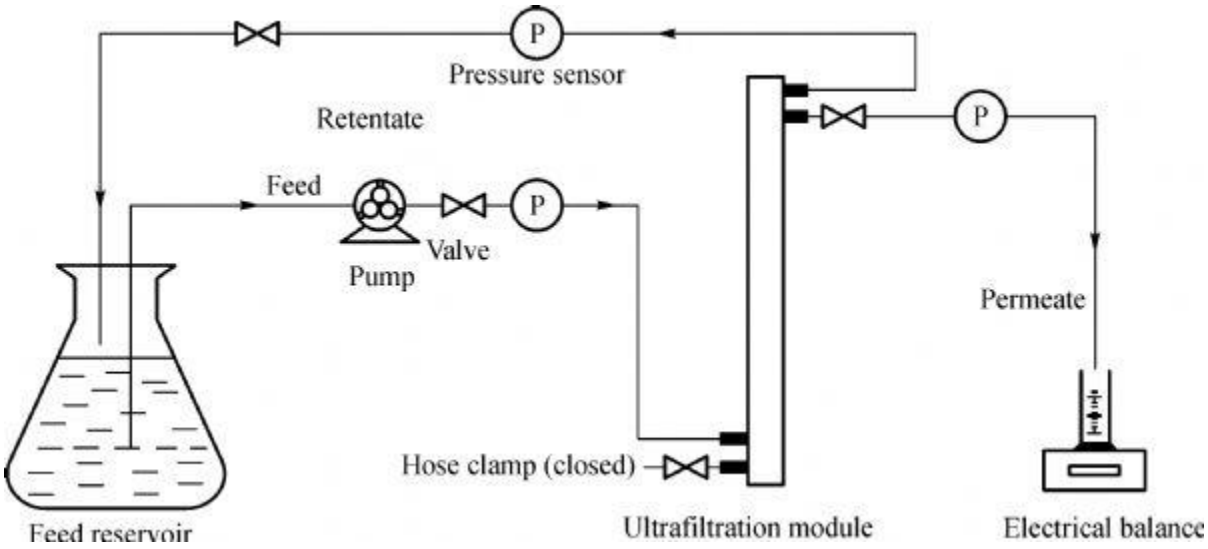


**Figure 5.** Schematic presentation of Tangential Flow filtration: Samples feed continuously through sample tube with the help of pump. During passing Solution is filtered through the membrane by incorporation of pressure. The resulting permeates accumulate differently whether retentate remain in the reservoir. Pressure valve and the electric balance give idea of current pressure and permeate amount respectively. [Adopted from, (Wang et al., 2015)]

### 4.10.5 Chromatographic purification

Spy Noro VLP, WT Noro VLP and Spyligase protein were purified using AKTA START chromatographic instrument (GE Healthcare, Chicago, USA). Favourable condition of washing the system tubing, column and equilibrating with binding buffer; sample application either using sample tubing or directly injecting into the column via sample loop; washing unbound protein and elution of protein in different fractions can be performed with AKTA START. It is also possible to monitor the concentration of protein by observing the absorbance of UV light at 280 nm in the software. The Specific UNICORN software also allowed to do some analysis of the collected data. Observing the chromatogram, we can estimate the protein containing tubes.

For Spy Noro VLP purification Hi-Load Q FF column was used for anion exchange chromatography. It is important to consider the isoelectric point (PI) of the protein. At

isoelectric point the protein net electrical charge is neutral (Novák and Havlíček, 2016). The PI of Spy Noro VLP was 5.6 and pH of phosphate buffer was 7, which allow binding of protein to the anion exchange column.

On the other hand, C-terminally polyhistidine tagged i.e. His-tagged Spyligase was separated by using the Ni-resin affinity column chromatography. This peptide tag is used as a powerful tool in the protein purification with the help of the immobilised metal ion and affinity chromatography. The main mechanism is that transition metal ions immobilised with a matrix of resin and another part form the coordination bond with amino acids side chains. Among other transition Ni ions show the best affinity binding with histidine. It is very easy to wash the column to remove the contaminants and elute the protein by just adjusting pH or incorporating free imidazole in the column. We have used elution buffer containing imidazole which competes with the metal ions and separates the proteins. It is possible to achieve 100 folds more protein which is >95% pure comparing to older methods.(Kang et al., 2014).

### 4.10.6 Dynamic light scattering analysis

Dynamic light scattering is one of the methods of defining a protein hydrodynamic diameter (size) and particle-size distribution based on volume. The method principle is that small particles move faster than the larger particles due to Brownian motion and if other parameters such as temperature and solvent viscosity are known, the hydrodynamic diameter of the particle can be determined by measuring the speed of particles in a liquid. When light beam from the monochromatic light source of the DLS instrument is directed to the sample contained cuvette, the particles in the sample scatter light (Figure 6A). The detector of the instrument detects the motion of the particles in the solution and give a calculation about the polydispersity and hydrodynamic diameter of protein and other molecules.

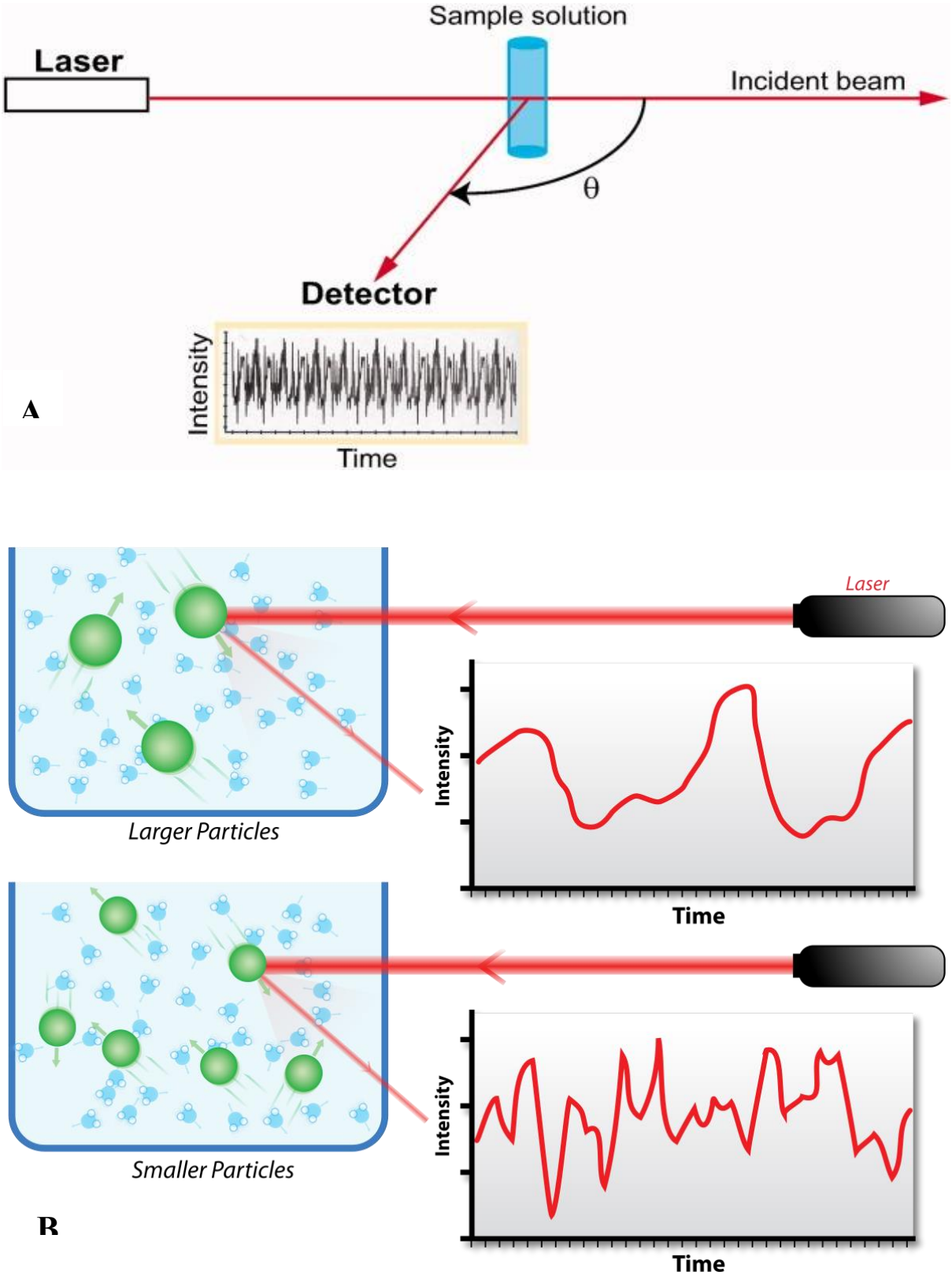


**Figure 6.** Principle of dynamic light scattering. **(A)** Schematic setup of a DLS system. Laser beam is the monochromatic light source which is directed to the sample. Protein molecules in the sample reflect light and are scattered in different directions with different angle. Detector detects the intensity of light as the function of time. **(B)** Large particles move slower than Small

particles. Histograms showed the movement of larger (up) and smaller particles (down). [The figure is modified from (Stetefeld et al., 2016)].

For the analysis of the hydrodynamic size and polydispersity index of the purified WT Noro VLP and Spy Noro VLP we have used DLS (using Zetasizer Nano ZS, Malvern Instruments, Worcestershire, US). This instrument uses a HeNe gas laser with wavelength 633 nm. The computer operated specific software gives us results of the hydrodynamic diameter of the sample. (Figure 6B). Before using this, we have made our specific predefined standard operating procedure (SOP) for the proteins and applied 25℃ temperatures. 173 degrees scattering angle was used in the measurement.

# 5 Results

## 5.1 Production of the Spy Noro VLP and WT Noro VLP in insect cells

After production of P1, P2 and P3 BV stocks in Sf-9 cells (Mehalko and Esposito, 2016), Spy Noro VLP and WT Noro VLP were produced in Hi-5 and TNI-FNL-Hi-5 cells. Based on amino acid sequence the molecular weight of full-length Spy Noro VLP and WT Noro VLP VP1 capsid proteins were 61 kDa and 59 kDa respectively (Figure 3A, 3B). However, Noro VLPs appear in double bands because of the production of the full length VP1 capsid protein in eukaryotic cells leads to formation of N-terminal posttranslational truncation of the protein. Therefore a heterogeneous mixture of full length (59 kDa) and truncated (57 kDa) proteins formed (Mallagaray et al., 2019). Approximately 57 and 61 kDa protein bands of Spy Noro VLP (Figure 7A); 57 and 61 kDa protein bands of WT Noro VLP (Figure 7B) were detected from SDS-PAGE analysis with a stain free detection system.

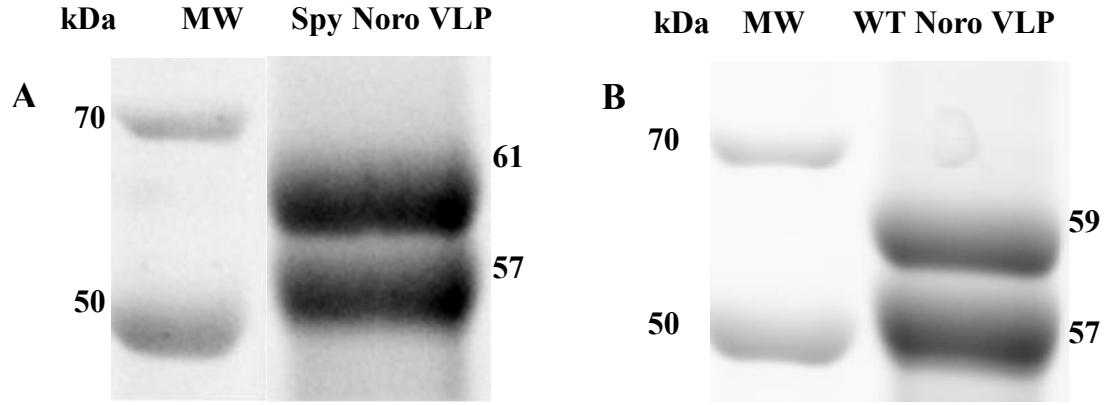


**Figure 7.** Stain free SDS-PAGE gel images of Spy Noro VLP and WT Noro VLP double bands**. (A)** The supernatant sample of Spy Noro VLP expressed in Hi-5 cells. Upper band of Spy Noro VLP is 61 kDa and lower one is 57**. (B)** Supernatant sample of WT Noro VLP double bands in TNI-FNL-Hi-5 cells. Upper band is approximately 59 kDa and lower one 57 kDa. MW lane shows the molecular weight marker.

## 5.2 Spy Noro VLP and WT Noro VLP production optimization

Cell lines derived from lepidopteran hosts such as *Spodoptera frugiperda* have commonly been used for the production of baculoviruses, while *Trichoplusia ni* cell lines have been shown in several cases to out-perform these cell lines for production yield to secreted proteins (Mehalko and Esposito, 2016). From previous study of our group it was found that optimal production efficiency for Spy Noro VLP is reached when Hi-5 cell cultures are set up at a density of 2 x $10^6$ cells/ml and the cells are infected with BV P2 stock at a multiplicity of infection (MOI) of 1. WT Noro VLP (GenBank ID: AFV08795) has been produced with a MOI of 1 with high

yield in Sf-9 cells (https://www.ncbi.nlm.nih.gov/pubmed/21854823, 20. 12.18). It was found that both, WT and Spy Noro VLPs production rates was higher in Hi-5 cells than in Sf-9 cells. Therefore, in this study we tested whether the VLP production rate could have been further increased in TNI-FNL-Hi-5 cell. Different volumetric ratios of WT Noro and Spy Noro VLP BV stocks were used in the infection of Hi-5 and TNI-FNL-Hi-5 cells. However, the production rate was substantially higher for both VLPs in Hi-5 cells than FNL-Hi-5 cells (Figure 8.) Volumetric ratio 1:50 of BV stocks in Hi-5 cells was chosen as the preferred production concentration for WT Noro VLP (Figure 8., Lane 4) and Spy Noro VLP (Figure 8., lane 10). Most of the VLP proteins were found in the extracellular supernatant sample whereas the intracellular pellet sample contained very little VLP (data not shown).

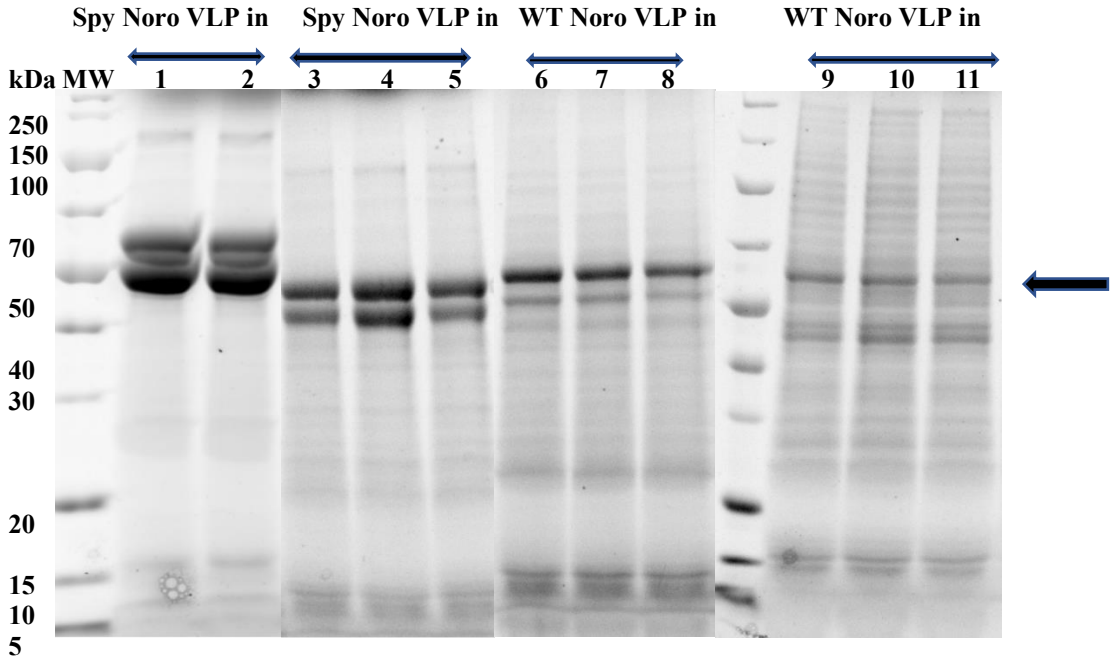


**Figure 8.** Selection of best cell line for Spy Noro VLP and WT Noro VLP production. SDS-PAGE gel images from test productions of the Spy Noro VLP and WT Noro VLP protein in Hi-5 cells and TNI-FNL-Hi-5 cells. MW lane shows molecular weight marker, 1and 2 are the supernatant sample of Spy Noro VLP in Hi-5 cells in 1:50 and 1:100 volumetric ratio (arrow mark showing protein bands). Lane 3-5 are culture supernatant of Spy Noro VLP in FNL-Hi-5 cells at 1:50, 1:100 and 1:200 volumetric ratio respectively. On the other hand, 6-8 are supernatant samples of WT Noro VLP in Hi-5 cells at same ratio. Lane 9-11 showing the supernatant sample of WT Noro VLP in 1:50, 1:100 and 1:200 ratio respectively.

### 5.3 Purification of Noro VLP

#### 5.3.1 Spy Noro VLP purification

The Spy Noro VLP supernatant was first concentrated by tangential flow filtration (TFF) and 30% sucrose cushion pelleting and finally the dissolved pellets were purified using anion

exchange chromatography. In the chromatogram isocratic (one-step) elution showed the sharp elution peak in tube T16, T17 and T18 (Figure 9A). According to the densitometric analysis of gel image (Figure 9B), after complete purification we got approximately >95% pure protein. The amount of Spy Noro VLP from this purification was roughly 133 mg/l (based on BCA assay analysis).

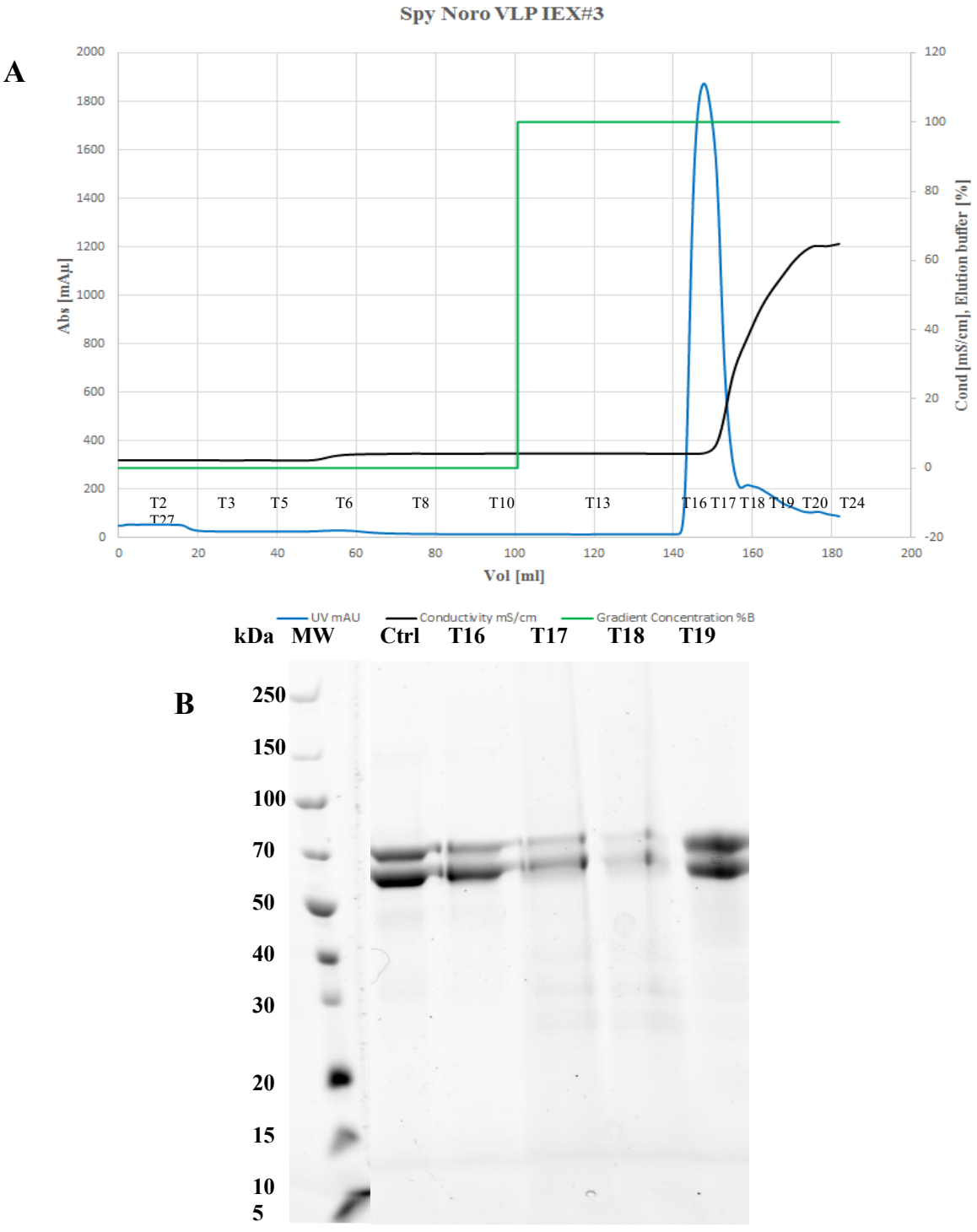

**Figure 9.** IEX purification of Spy Noro VLP. Spy Noro VLP IEX purification chromatogram **(A)** Blue line is indicating absorbance, green and black represent concentration of elution. buffer and conductivity respectively. Highest elution peak found in Tube T16, T17, T18 where most of the protein were eluted. **(B)** Stain free SDS-PAGE gel image of most concentrated fractions of Purified Spy Noro VLP. MW indicates molecular weight marker. From the left, control sample lane, sample from batch #3 (T19-T16). Image indicated the successful purification of Spy Noro VLP from the anion exchange chromatography using HiLoad 50 ml Q column.

### 5.3.2. Wild Type Noro VLP purification

WT Noro VLP purification was started with tangential flow filtration using AKTA Flux S and 30% Sucrose cushion pelleting. WT Noro VLP purification was completed with anion exchange chromatography. SDS-PAGE analysis of load, supernatant and pellet sample reveals the purity state of the WT Noro VLP. Chromatogram (Figure 10A) of WT Noro VLP purification showed the successful elution of protein. At 0.6 M elution buffer, most of the WT Noro VLP eluted from the column. Elution fractions F10-F12, F4-F9 and F13-F22 were pooled together and concentrated using VivaspinTurbo Ultrafilter. We obtained around 3.8 mg/l WT Noro VLP from this purification.

The final product of Spy Noro VLP was >95% pure and two fractions of WT Noro VLP were >50% and >95% pure (Figure 10C).

**A**

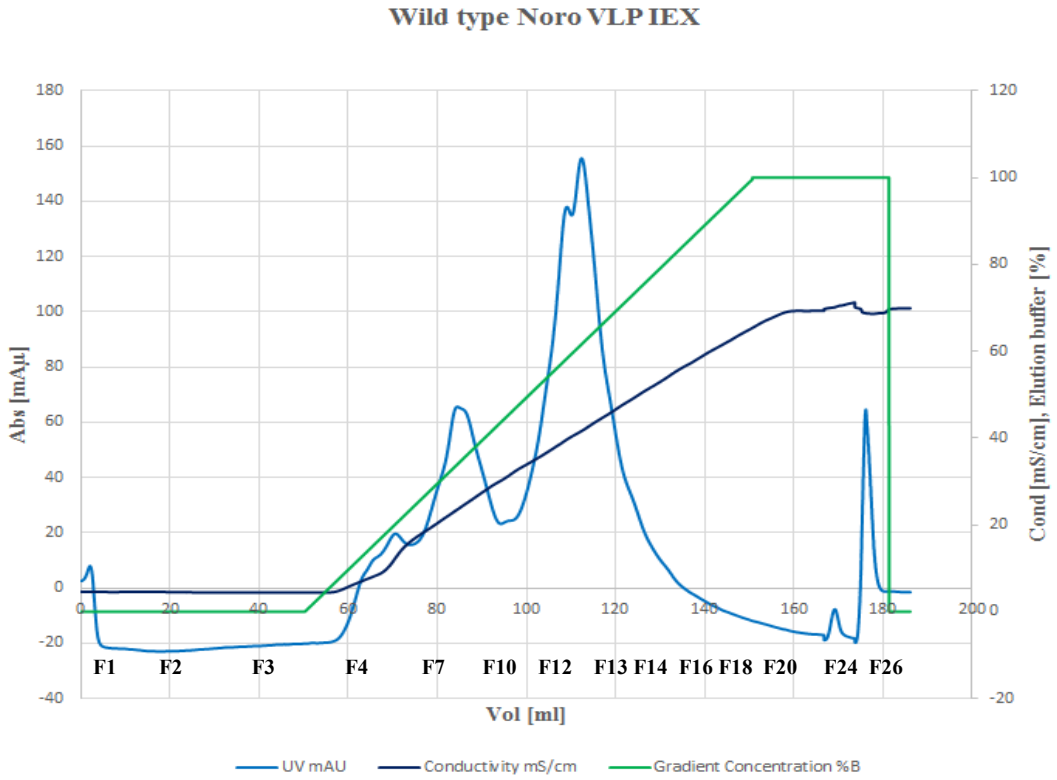

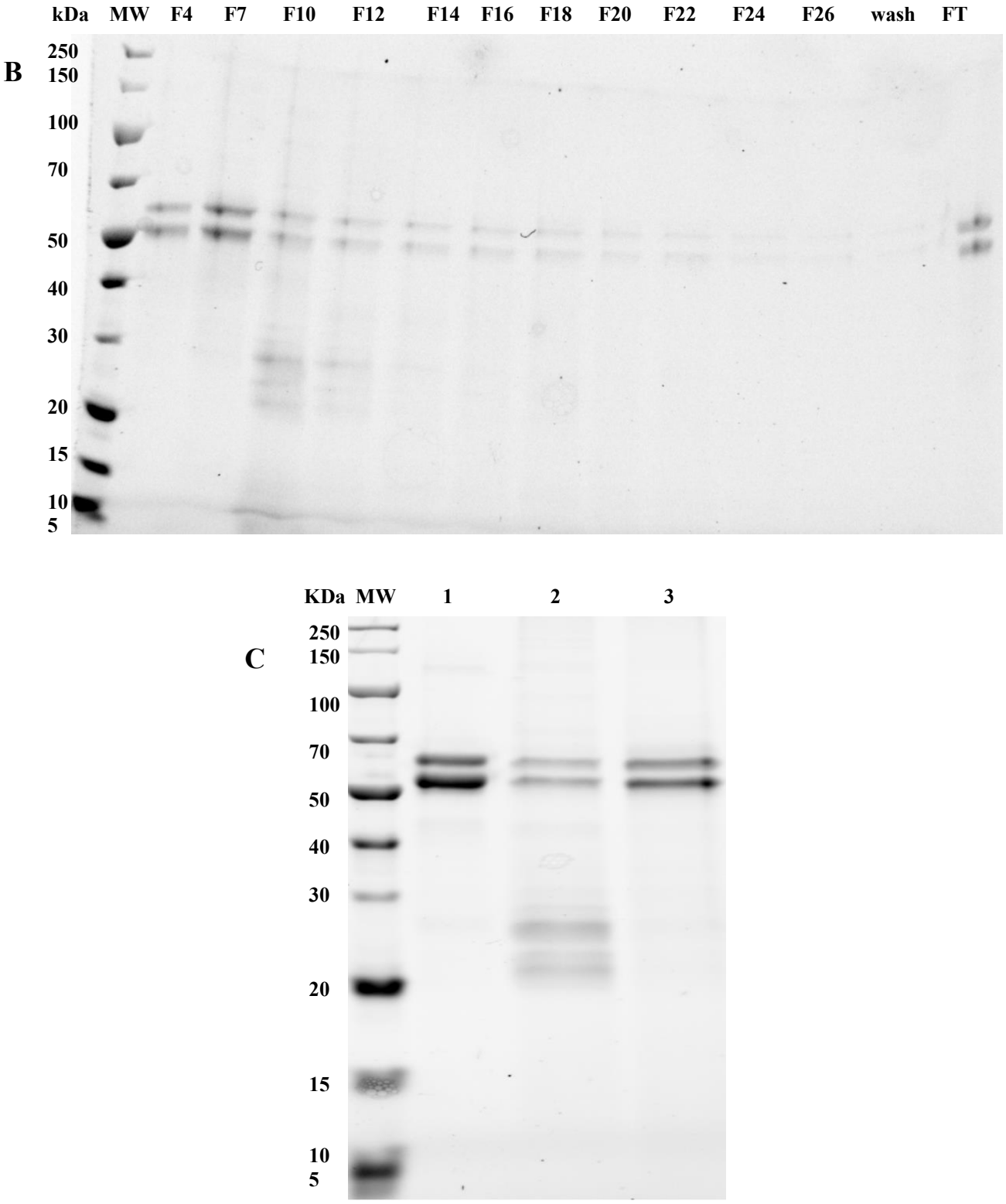


**Figure 10.** Wild type Noro VLP purification. **(A)** IEX purification chromatogram of WT Noro VLP. Blue line is showing the absorbance, green line buffer concentration and black line indicate conductivity. Selected locations of elution fractions are indicated in the figure. Raise of the elution buffer concentration increase the protein elution, seen from the blue absorbance peak. Most of the protein eluted in F13, F14, F15 around the highest peak. **(B)** Stain free SDS-PAGE gel image of WT Noro VLP samples. MW lane contains unstained molecular weight protein marker. F4-F26 are the elution fractions sample, and rest of the two lanes are from wash and 'FT' is the Flow through sample. **(C)** Final product of purified Spy Noro VLP and WT

Noro VLP. Lane 1 contains pure Spy Noro VLP, lane 2 contains WT Noro VLP (>50% purity), and lane 3 contains WT Noro VLP (>95% purity) from same batch.

### 5.3.3 Endotoxin removal from the protein

Endotoxin removing trial using nickel sepharose column (5 ml) for Spyligase was found to be effective. Slightly higher endotoxin than acceptable level was found for the purified Spyligase. Allowable limit of endotoxin in gene vector vaccine is 10 (EU/ml) whereas, <20 EU/ml in case of recombinant subunit vaccine (Brito and Singh, 2011). For a 20 g mouse maximum endotoxin level is 0.1 (EU/ml) during 1hour injecting time (Brito and Singh, 2011). Before endotoxin removal trial, 1873 EU/ml of endotoxin was measured in the Spyligase sample using Limulus amebocyte lysate (LAL) assay (Trivedi et al., 2003) whereas, after the triton X114 wash 98 EU/ml endotoxin was detected by using same method. Around 19 folds endotoxin reduction was possible by this method.

## 5.4 Production of Spyligase

### 5.4.1 Plasmid recovery

Bacterial stab containing transformed bacteria with plasmid pDEST14-Spyligase (Addgene plasmid #51722) was isolated in single colony. Then these colonies were inoculated in 200 ml Gluc-LB medium and following overnight incubation plasmid DNA was isolated by following the user manual of NucleoBond Midi plus EF (Loughborough, Leicestershire, UK).

### 5.4.2 Culture condition optimization and purification of Spyligase

For optimal production of Spyligase, culture temperature of BL21star DE3 bacteria strain was optimized. According to the amino acid sequence, molecular weight of the His-Tagged Spyligase is 11.47 kDa. In the gel a protein corresponding to this size was found that bind to the Ni-NTA-resin (Figure 11). Different production temperatures (18, 25 and 37°C) were compared for Spyligase production and we found that BL21 Star DE3 strain produces the highest amount of protein at 18°C (Figure 11). Protein production was highest using 1 mM IPTG at OD≈0.6.

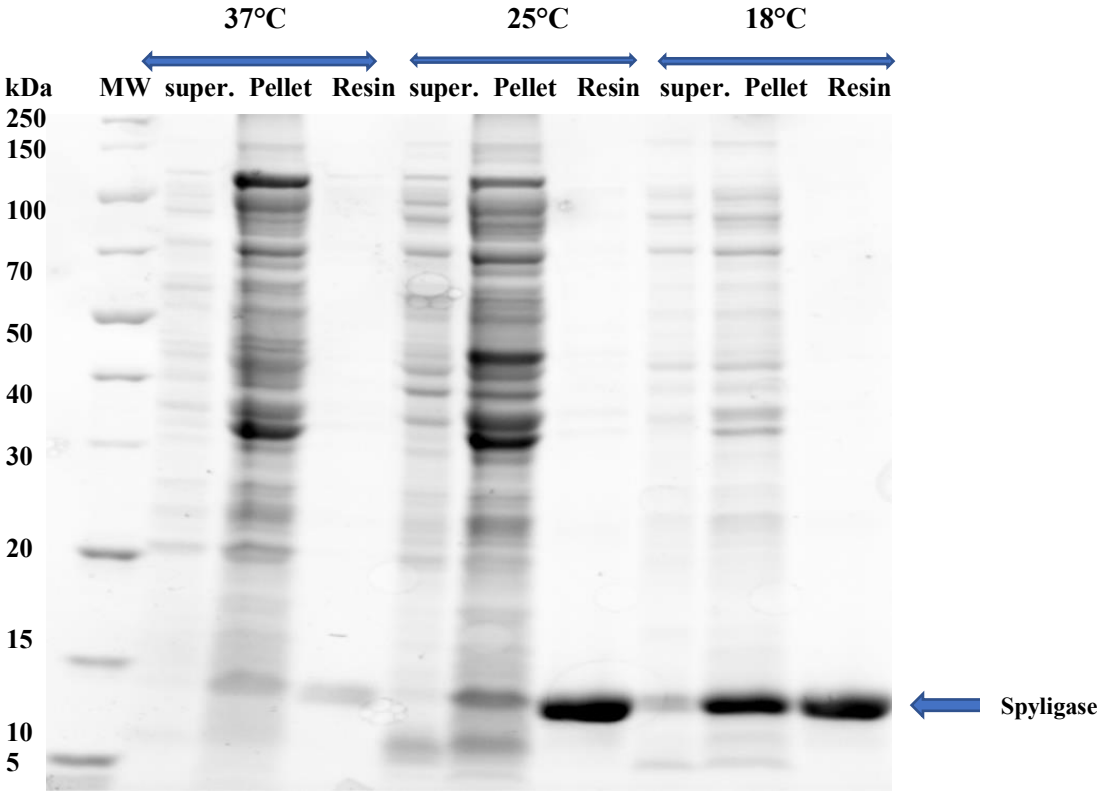


**Figure 11. Production temperature optimization of Spyligase.** Production temperature optimization. SDS-PAGE gel was showing the intense band in resin and pellet sample at 18°C but at 25°C, intense protein band found in resin sample only. Overall 18°C have been showing the best culture temperature for Spyligase production. Lane MW is the molecular marker, Super. is indicating supernatant sample, pellet contains the bacterial pellet samples and resin contain the resin bounded Spyligase.

### 5.4.3 Large-scale Spyligase production and purification

When optimal production temperature for Spyligase was determined, a large-scale production (1-liter production volume) for Spyligase protein was produced and purified with IMAC. Using 250 mM imidazole in elution buffer, we were able to elute most of the Spyligase protein. SDS-PAGE analysis of the elution fractions and other collected samples show that most of the impurities did not bind to the column and passed with flow through. A prominent elution peak was detected in the chromatogram (Figure 12A). SDS-PAGE gel (Figure 12B) analysis assure purity of protein and approximately >95% pure Spyligase protein with yield of 84 mg/lwas obtained.

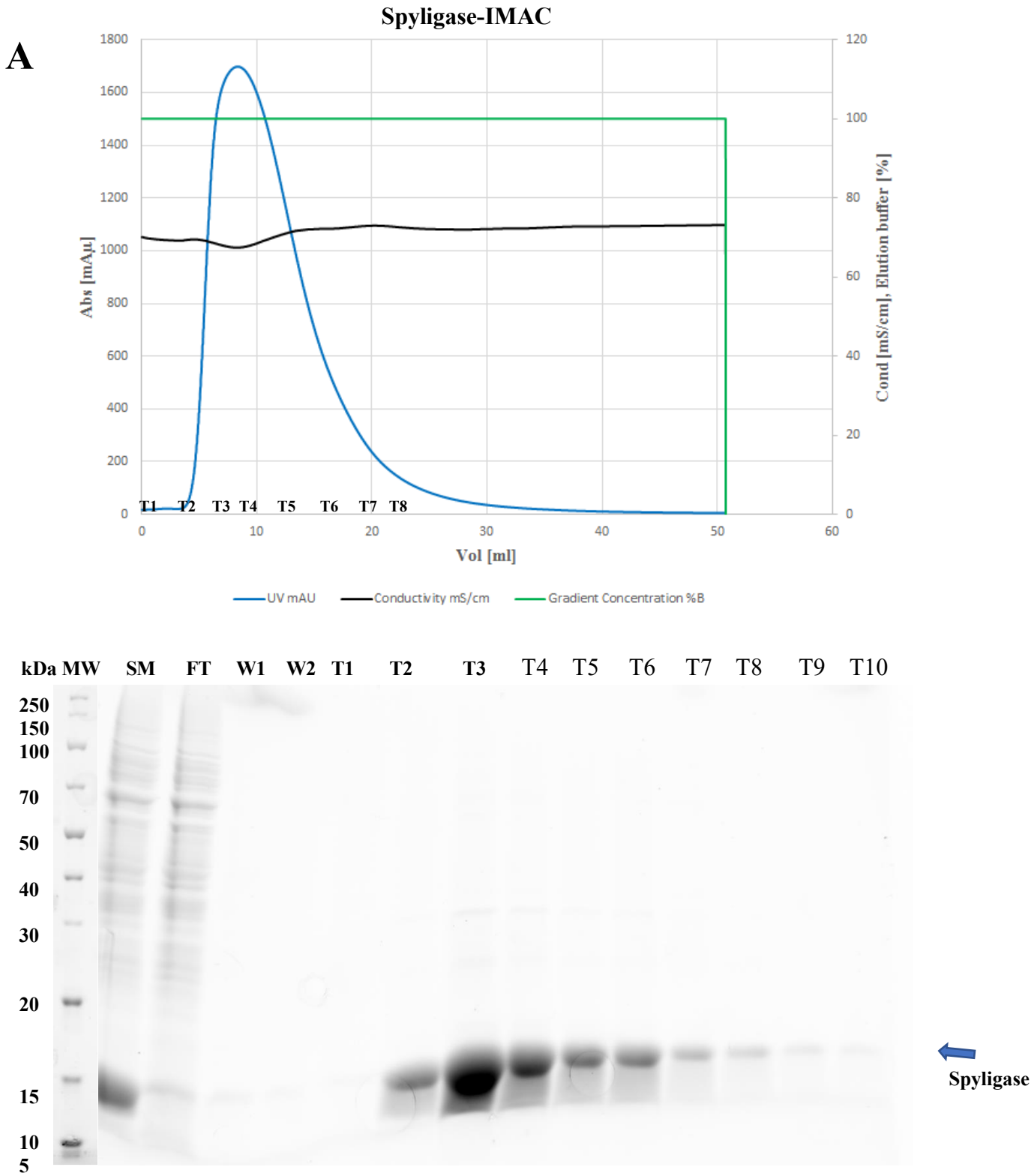


**Figure 12. IMAC purification of Spyligase. (A)** Elution chromatogram of Spyligase sample. Blue line shows the Absorbance at 280 nm wavelength. Black line shows the conductivity of the solution and green line shows buffer B percentage (%). Locations of selected elution fractions are indicated in the figure. Clear absorbance peak was (Blue line) obtained and T2, T3, T4 contains most of the protein. **(B)** Stain free SDS-PAGE gel image is showing the elution

fractions from HisTrap Q FF crude column. MW is for Molecular weight marker. SM is the starting material for IMAC purification, whereas, FT and W indicating flow through and wash sample and T1-T10 are elution fractions. T3 elution fraction are showing the most intense band and most of the fractions are clear.

### 5.5 Dynamic light scattering analysis

Dynamic light scattering analysis was done to estimate the size of Spy Noro VLP and WT Noro VLP. Analyses were done in PBS buffer. According to DLS analysis 100% of Spy Noro VLP had an average hydrodynamic diameter of 51 nm (Figure 13A). 100% of pure WT Noro VLP and 95% of less pure WT Noro VLP had an average hydrodynamic diameter of 53 nm (Figure 13B) and 32 nm (Figure 13C) respectively. Polydispersity index (Pdl) of Spy Noro VLP, pure WT Noro VLP and less pure WT Noro VLP were 0.099, 0.209 and 0.269 respectively.

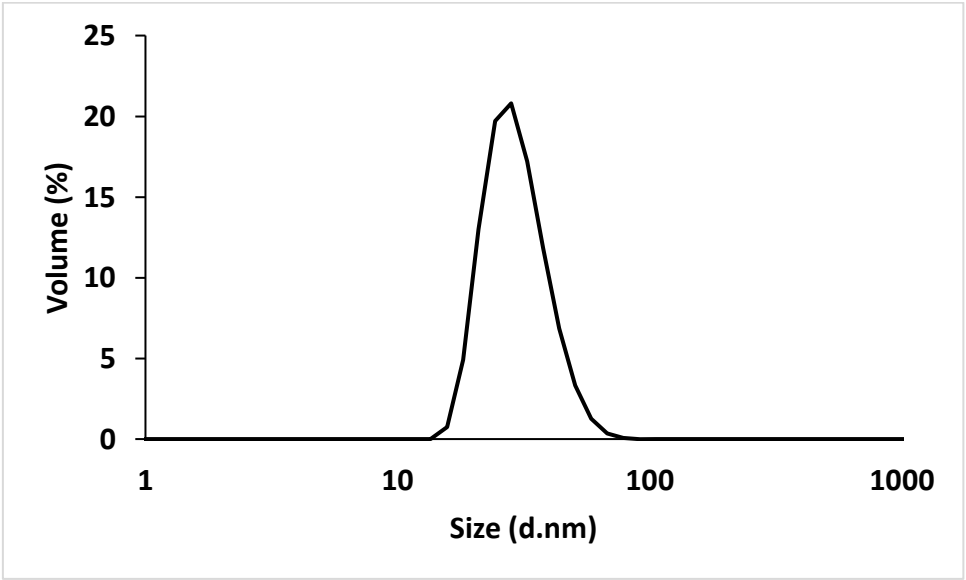


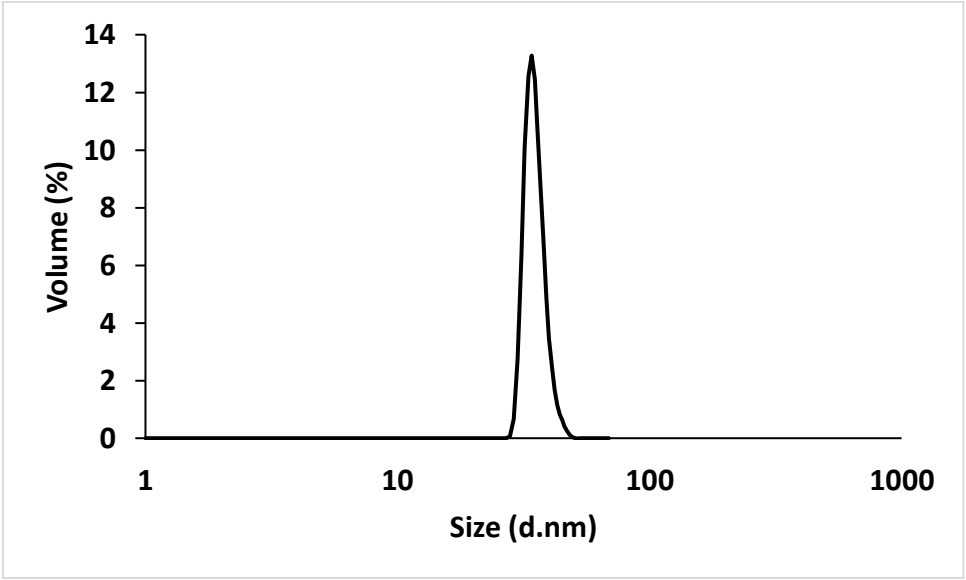

C

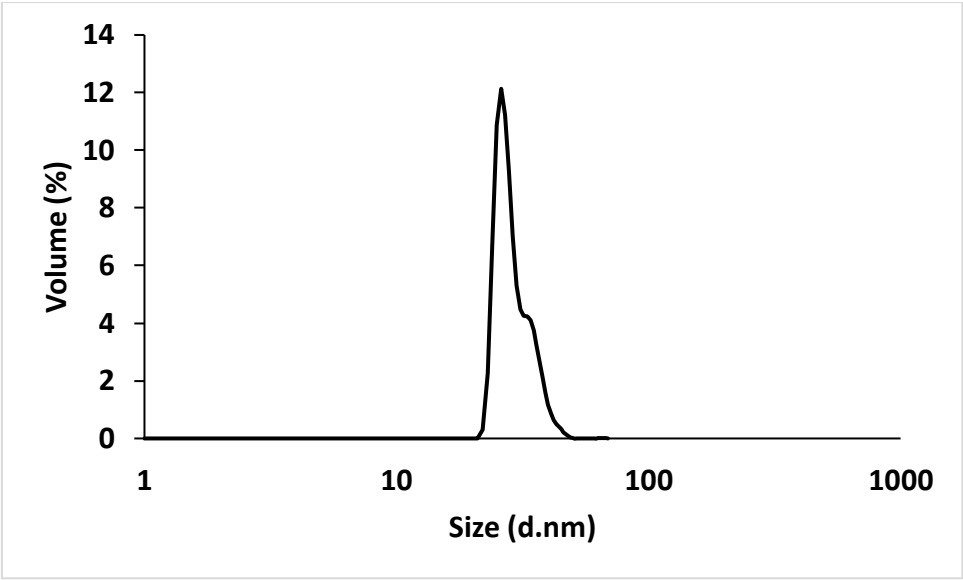


**Figure 13.** Size distribution of VLPs by DLS method. **(A)** The average size of Spy Noro VLP was 51 nm. **(B)** The average size of pure WT Noro VLP was 53 nm. (**C**) Average size of less pure WT Noro VLP was 32 nm.

### 5.6 Conjugation reaction of Spy-Tagged Noro VLP and K-Tagged antigen

PCT buffer containing 40 mM phosphate, 20 mM citric acid buffer and 1.5 M tri-methyleamine N-oxide as protein stabilizer was used for conjugation of Spy-Tagged Noro VLP and K-Tagged antigen. During SDS-PAGE analysis using 12% SDS-PAGE gel it was very difficult to find the difference between conjugated and non-conjugated antigen and Spy Noro VLP (Figure 14A). The molecular weight of the synthetic K-Tagged M2e peptide is only 3.73 kDa. Therefore, SDS-PAGE gel was western blotted and stained with anti-M2e mouse monoclonal antibody (Figure 14B). An intense band of conjugated antigen with Spy Noro VLP was detected with M2e mAb. We were able to demonstrate that K-Tagged M2e was able to conjugate with the spy-tagged Noro VLP.

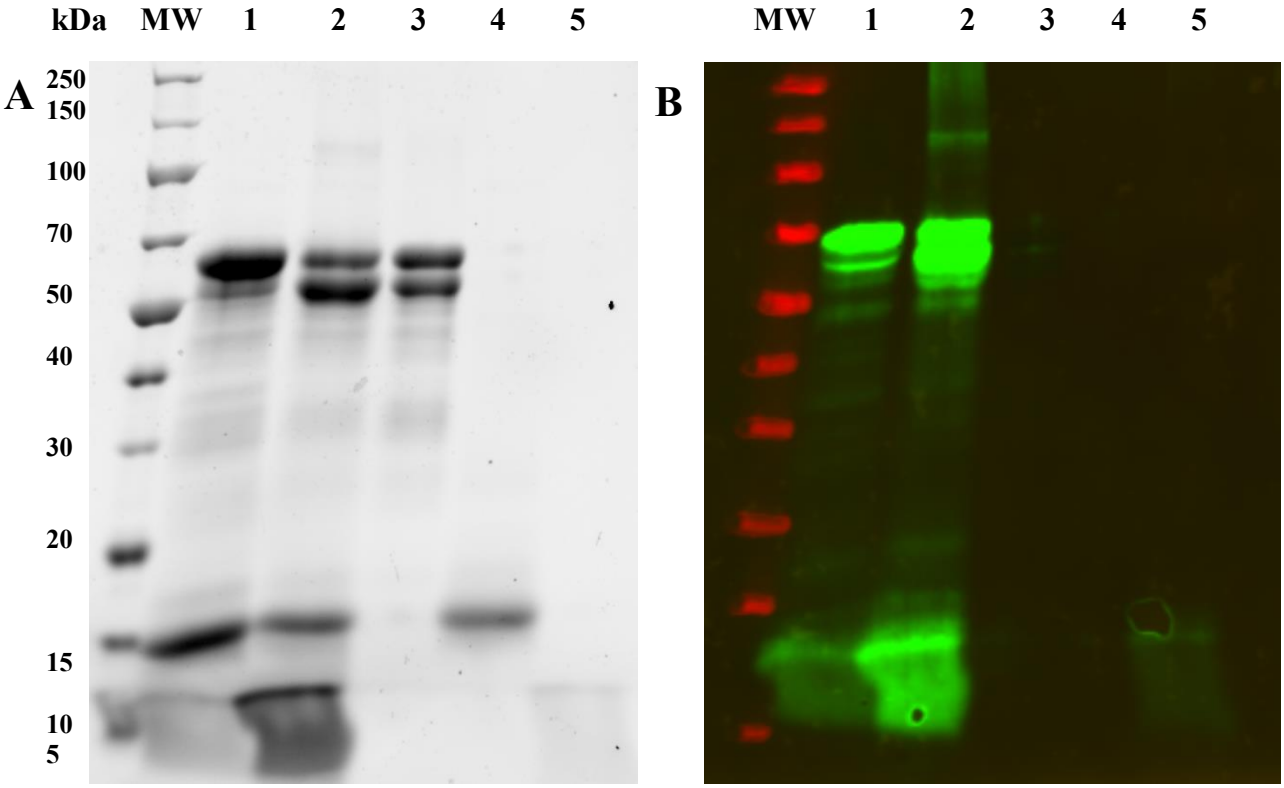


**Figure 14:** Conjugation reaction of K-Tagged M2e and Spy Noro VLP catalyzed by Spyligase. **(A)** Analysis of conjugated Spy Noro VLP and K-Tagged M2e compared to respective vaccine components alone in SDS-PAGE gel stained with stain free technology. MW: molecular weight marker, lane 1-5 contains conjugation reaction control (sample from previous successful reaction of Spy Noro VLP, K-Tagged M2e antigen and Spyligase), conjugation reaction sample (Spy Noro VLP, K-Tagged M2e antigen and Spyligase), Spy Noro VLP control; Spyliagse control and K-Tagged M2e antigen control respectively. **(B)** followed by western blotting analysis stained with M2e mAb.

# 6 Discussion

In this study VLP production was tried in Hi-5 insect cells and another strain of Hi-5, TNI-FNL-Hi-5 cells. Previously in other studies scientist have reported successful production of different VLPs using Hi-5 cells (Lin et al., 2015). We found that, Hi-5 cells were more efficient in WT Noro VLP and Spy Noro VLP production than TNI-FNL-Hi-5 cells. 5-6 dpi was found best for maximum production of VLPs.

During this study several steps of the VLP production and purification were optimized in order to produce highest possible amount of protein. In the first batch of Spy Noro VLP, protein purification was not successful and most of the proteins did not bind the chromatography column (VLP was found in the pellet, wash and flow through fractions). Unbound protein in the flow through sample might be happen because of insufficient column capacity, inappropriate buffer pH and inaccurate conductivity. To resolve the condition, conductivity of sample was reduced to 3.5 µS/cm by adding sample dilution buffer and anion exchange chromatography was performed with a larger column. HiLoad QA FF 50 ml column was used which would be another important reason to produce higher amount of protein. In this big column, proteins were easily captured due to its large surface area, moreover, moderate conductivity make it easy for protein to bind to the column. That's why column capacity including sample conductivity found effective in both Spy Noro VLP and WT Noro VLP IEX purification. Koho et al, (2014) reported successful purification of VLP using TFF, sucrose cushion and IEX, where they found 95% pure protein. Similarly, in this study >95% pure protein was obtained using the TFF and sucrose cushion and IEX purification. Finally, we were able to produce approximately 133 mg of Spy Noro VLP protein from 1 L of production culture. Whereas, Koho et al. (2015) have shown only 1.5 mg/l yield for purified His-Tagged Noro VLP.

In case of WT Noro VLP purification, we obtained 3.8 mg/l pure protein. Koho el al. (2012) have reported 100 mg/l yield of a different strain of WT Noro VLP (using PEG precipitation and sucrose gradient). In the beginning, WT Noro VLP purification was performed with TFF, sucrose cushion pelleting and cation exchange chromatography. However, the cation exchange purification was found to be unsuccessful, since most of the VLPs did not bind the column. After replacing the cation to anion exchange chromatography, it was found effective but

purified protein amount was low. Still it is necessary to optimize the production conditions for WT Noro VLP for a higher production rate.

In the SDS-PAGE gel image there was faint band in some of the lane of Spy Noro VLP. These were found near to the 120 kDa protein bands and only in the highly concentrated elution fractions of the Spy Noro VLP. Though they were not seen in the load sample, this indicated the dimer formation (Heinimäki et al., 2017) of VLP that could not be denatured with heating at 100°C for ten minutes in the presence of beta-mercaptoethanol. Proper sample mixing with protein denaturing agent, careful heating at 100°C for 10-12 minutes and use of less amount of protein in each well could be a solution to avoid dimer formation in the sample.

In all stages of production and purification of WT Noro VLP and Spy Noro VLP, a double band was detected in the SDS-PAGE gel. Two bands were adjacent to each other between the (50-70) kDa protein marker bands. The molecular weight of both VLPs support the double bands near to that area of the gel image and it was expected (Figure 7A, 7B). These bands were due to the post translational excision of Noro VLP VP1 protein. White et al., (1997) have reported thirty-four N-terminus amino acid base cleavage after production of the Noro VLP VP1 protein. In a different study it was tried to express VP1 protein without first thirty-four amino acids, which was concluded with low production level and non-forming VLPs (Bertolotti-Ciarlet et al., 2002). Even though N-terminal amino acid truncation strategy of VP1 protein and their importance in VLP formation is still a mystery but it is out of dispute that full length VP1 protein production is essential for full forming VLPs (Koho et al., 2012).

Although, UV/Vis spectrophotometer was used in quantitation of proteins during the purification process, it was found not to be accurate. Therefore, the final concentration of all proteins was measured using BCA analysis method. PEG precipitation with sucrose gradient was showing higher yield but it was not ideal to use PEG for vaccine production because it could mask the VLP surfaces (Hinrichsen et al., 2017). Tangential Flow filtration helps to fasten the purification method but is unprotected of contamination from air. At the same time, Ultracentrifugation process is good enough for small scale purification, but large-scale purification is very time consuming. However, TFF and ultracentrifugation and IEX was applied successfully in the current study for the purification of WT Noro VLP and Spy Noro VLP. So, efficient purification of WT Noro VLP and Spy Noro VLP are possible by using TFF, ultracentrifugation and anion exchange chromatography.

Recombinant protein production yield in bacteria is affected by growth temperature, optical density and IPTG concentration (Mühlmann et al., 2017). Spyligase production was optimized in BL21 Star DE3 *E. coli* strain. The production rate was found higher at 18 ºC compared to 25ºC and 37ºC in small scale and large-scale culture as well. Optical density may cause a great difference to the production. At $OD_{(600)} \approx 0.4$ including 1mM IPTG Spyligase production was best. Constant shaking of the culture for gas exchange was an important feature of producing maximum amount of protein (Mühlmann et al., 2017).

Purified Spyligase protein did not contain any other protein bands and was pure enough for vaccine production trial. However, after measuring endotoxin levels in the Spy Noro VLP, WT Noro VLP and Spyligase we found higher endotoxin levels than the allowable amount for vaccines in animal trials. One of the possible reasons would be the *E. coli* bacteria itself in case of Spyligase production and another bacterial contamination in any purification step even though all purification steps were done with aseptic techniques. Therefore, it is still unknown where these endotoxins came in WT Noro and Spy Noro VLP.

To remove endotoxins from the purified Spy Noro VLP three different strategies were tried. Firstly, IEX purification using same protocol with longer washing step which was not effective. Secondly, by conjugating the antigen to Spy Noro VLP and applied to IEX, this was also not effective as approximately same amount of endotoxin found after measuring. Finally, Triton X114 was used to remove the endotoxin, but most of the protein eluted in the washing step with triton X114 and after that, washing with binding buffer. It is still in shadow how to remove endotoxin from Spy Noro VLP. On the other hand, in case of Spyligase IMAC purification, His-Tagged Spyligase bound strongly to the column prior to sample application and 1 extra washing step with 0.1% triton X114 removed the endotoxin. It was found very effective to remove endotoxins from his-tagged protein. It would be possible to remove endotoxins more efficiently by increasing triton X114 washing step one or two round.

Influenza M2e is a potential vaccine candidate for some essential aspect. M2e is a very conserved sequence (Sutton et al., 2017), mutation rate is lower than the HA and NA matrix proteins (Kolawole et al., 2017). Although, M2e is very small peptide and solely not so immunogenic, VLP platform should make it more robust (Lee et al., 2018). To make an universal vaccine by using this peptide antigen it is necessary to conjugate it with VLP platform which would work better as vaccine candidate (Deng et al., 2015). In this study, >95% pure K-Tagged M2e synthetic peptide was used. Previous study revealed that, M2e works better after dissolving in PCT buffer which contains thrimethylamine N-oxide protein stabilizer (Siegmund

et al., 2016). Moderate precipitation was found in the reaction tube which is still a problem to be solved.

The K-Tagged M2e antigen is 32 amino acid peptides with 3738.4 Dalton molecular weight. After mixing the antigen and Spy Noro VLP and Spyligase, proper conjugation identification is difficult using only SDS-PAGE analysis. Band mobility shift is very minor in the SDS-PAGE. For that reason, M2e specific monoclonal antibody was used to analyze in western blot method. Odyssey image technology revealed the conjugation in the western blot image near to the specific molecular band.

Reaction of K-Tag, Spy-Tag and Spyligase is slower than the Spy-Tag and Spy-Catcher conjugation reaction (Fierer et al., 2014). In previous study, conjugation reaction efficiency was found only 30-50 % for conjugating IgG1-Fc with 6-carboxytetramethylrhodamine by using Spy-Tag and K-Tag, which is moderate (Veggiani et al., 2014). Although Spy-Tag and Spy-Catcher are active in different temperatures, a wide range of pH (5-8) and can tolerate detergents in the reaction, it is necessary to optimize the proper reaction conditions and buffers as well (Veggiani et al., 2014). In case of Spy-Tag and K-Tag conjugation works better at 4ºC (Siegmund et al., 2016).

Still we need to optimize and find the proper way of separating unconjugated and conjugated K-Tag, Spy-Tagged VLPs, which is necessary for animal trial. Moreover, time series conjugation reaction and reaction efficiency of peptide tags need to justify.

In last three decades extensive research in this field of universal influenza vaccine production is going on. Application of different technology like using VLP, easy production ability of viral proteins and safe vaccine prototype are some impressive outcomes of the research. However, a universal vaccine to protect pandemic in future is still far away. Due to the limitation on targeting HA, NA protein, targeting conserved sequence such as M2e is getting more attention. Using K-Tag, Spy-Tag including Noro VLP platform hopefully will accelerate to find an ultimate solution against influenza in near future.

# 7 Conclusion

Spy Noro VLP and WT Noro VLP were successfully produced in different insect cell lines. Comparatively, Hi-5 cells were found to be more efficient for producing both Spy Noro VLP and WT Noro VLP than TNI-FNL-Hi-5 cells. A volumetric ratio of 1:50 was used to produce the VLPs in Hi-5 cells. From 1 L large scale Spy Noro VLP production, approximately 133 mg pure VLP was obtained after successful purification using TFF, 30% sucrose cushion pelleting by ultracentrifugation and anion exchange chromatography. Applying same purification methods as like Spy Noro VLP, 3.8 mg/l pure WT Noro VLP was obtained. The purity of Spy Noro VLP was > 95% and WT Noro VLP was > 95% and >50%. In the DLS analysis the hydrodynamic diameter of Spy Noro VLP, >95% pure WT Noro and >50% pure WT Noro VLP were measured 51 nm, 53 nm and 32 nm respectively.

Production of Spyligase was efficiently done in *E. coli* strain (BL21 Star DE3). After optimizing culture condition, 18 ºC was found the best culture temperature. Using 1 mM IPTG in optimum temperature, from 1-liter production culture, 86 mg and >95% pure protein was gained after IMAC purification. Endotoxins of Spyligase were 19 folds reduced by using 0.1 % Triton X114 extra washing step in the IMAC purification method.

After successful purification and dialysis of Spy Noro VLP and Spyligase they were mixed with M2e antigen and incubated at 4 ºC. SDS-PAGE and western Blot analysis proved the isopeptide bond formation between Spy-Tag and K-Tag by dint of Spyligase, which was identified by antibody recognition process. The next step would be to analyze conjugation efficiency, time series conjugation reaction and removal of unbound antigen before proceeding to animal trial with M2e decorated Spy Noro VLP vaccine.

# 8 References


Akahata, W., Yang, Z., Andersen, H., Sun, S., Holdaway, H. A., Kong, W., Nabel, G. J. (2010). A VLP vaccine for epidemic chikungunya virus protects non-human primates against infection. *Nature Medicine, 16*(3), 334-338. doi:10.1038/nm.2105

Al-Tubuly, A. A. (2000). SDS-PAGE and western blotting. *Methods Mol Med., 40*(4), 391-405.

Babapoor, S., Neef, T., Mittelholzer, C., Girshick, T., Garmendia, A., Shang, H., Burkhard, Peter. (2011). A novel vaccine using nanoparticle platform to present immunogenic M2e against avian influenza infection. *Influenza Research and Treatment, 2011*, 126794-12. doi:10.1155/2011/126794

Bertolotti-Ciarlet A., White, L. J., Chen R., Prasad, B. V., and Estes M. K. (2002). Structural requirements for the assembly of norwalk virus-like particles. *Journal of Virology, 76*(8), 4044-4055. doi:10.1128/JVI.76.8.4044-4055.2002

Biabanikhankahdani, R., Bayat, S., Ho, K. L., Alitheen, N. B. M., and Tan, W. S. (2017). *A* simple add-and-display method for immobilisation of cancer drug on his-tagged virus-like nanoparticles for controlled drug delivery. England: *Nature Publishing Group.* doi:10.1038/s41598-017-05525-4

Brady, J. P., Farber, P. J., Sekhar, A., Lin, Yi-H., Huang, R., Bah, A., Kay, L. E. (2017). Structural and hydrodynamic properties of an intrinsically disordered region of a germ cell-specific protein on phase separation. W*ashington: National Academy of Sciences.* doi:10.1073/pnas.1706197114

Bright, R. A., Carter, D. M., Daniluk, S., Toapanta, F. R., Ahmad, A., Gavrilov, V., Massare, M., Pushko, P., Mytle, N., Rowe, T., Smith, G., Ross, T. M. (2007). Influenza virus-like particles elicit broader immune responses than whole virion inactivated influenza virus or recombinant hemagglutinin. *Vaccine, 25*(19), 3871-3878. doi:10.1016/j.vaccine.2007.01.106

Brito, L. A., and Singh, M. (2011). Acceptable levels of endotoxin in vaccine formulations during preclinical research. *Journal of Pharmaceutical Sciences, 100*(1), 34-37. doi:10.1002/jps.22267

Brune, K. D., Leneghan, D. B., Brian, I. J., Ishizuka, A. S., Bachmann, M. F., Draper, S. J., .Howarth, M. (2016). Plug-and-display: Decoration of virus-like particles via isopeptide bonds for modular immunization. *Scientific Reports, 6*(1), 19234. doi:10.1038/srep19234

Burd, E. M. (2003). Human papillomavirus and cervical cancer. *Clinical Microbiology Reviews, 16*(1), 1-17. doi:10.1128/CMR.16.1.1-17.2003

Camper, D. V., and Viola, R. E. (2009). Fully automated protein purification. *Analytical Biochemistry, 393*(2), 176-181. doi:10.1016/j.ab.2009.07.009

Cao B., Xu H., Yang M., Mao C. (2018). . Virus-based cancer therapeutics for targeted photodynamic therapy. in: Wege C., lomonossoff G. (eds) virus-derived nanoparticles for advanced technologies. methods in molecular biology, .and nbsp; *Humana Press, New York, NY., vol 1776*

Centre for disease control and prevention. (2019). and nbsp; influenza (flu): Preliminary burden estimates. https://www.cdc.gov/flu/about/burden/preliminary-in-season-estimates.htm

Chan, W., Verma, C. S., Lane, D. P., and Gan, S. K. (2013). A comparison and optimization of methods and factors affecting the transformation of escherichia coli. *Bioscience Reports, 33*(6) doi:10.1042/BSR20130098

Cho, K. J., Schepens, B., Seok, J. H., Kim, S., Roose, K., Lee, J., Rousseau, F. (2015). Structure of the extracellular domain of matrix protein 2 of influenza A virus in complex with a protective monoclonal antibody. United States: *Katholieke Universiteit Leuven*. doi:10.1128/JVI.02576-14

Chou, Y., Heaton, N. S., Gao, Q., Palese, P., Singer, R., and Lionnet, T. (2013). Colocalization of different influenza viral RNA segments in the cytoplasm before viral budding as shown by single-molecule sensitivity FISH analysis. *PLoS Pathogens, 9*(5), e1003358. doi:10.1371/journal.ppat.1003358

Cimica, V., and Galarza, J. M. (2017). Adjuvant formulations for virus-like particle (VLP) based vaccines. *Clinical Immunology, 183*, 99-108. doi:10.1016/j.clim.2017.08.004

De Vincenzo, R., Conte, C., Ricci, C., Scambia, G., and Capelli, G. (2014). Long-term efficacy and safety of human papillomavirus vaccination. *International Journal of Women's Health, 2014*(default), 999-1010. Retrieved from https://doaj.org/article/b23048c417a4499eb6be20f544e48830

Debbink, K. (2015). Virus-like particles as future norovirus vaccines. *Future Virology, 10*(8), 1-3. doi:10.2217/FVL.15.63

Deng, L., Cho, K. J., Fiers, W., and Saelens, X. (2015). M2e-based universal influenza A vaccines. *Vaccines*, 3(1), 105-136. doi:10.3390/vaccines3010105

Ding, X., Liu, D., Booth, G., Gao, W., and Lu, Y. (2018). Virus-like particle engineering: From rational design to versatile applications. *Biotechnology J.* 13(5), 15-25 doi:10.1002/biot.201700324

Ebrahimi, S., and Tebianian, M. (2011). Influenza A viruses: Why focusing on M2e-based universal vaccines. *Virus Genes, 42*(1), 1-8. doi:10.1007/s11262-010-0547-7

Englander, S. W., and Mayne, L. (2014). The nature of protein folding pathways. *Proceedings of the National Academy of Sciences of the United States of America, 111*(45), 15873-15880. doi:10.1073/pnas.1411798111

Fiers, W., De Filette, M., El Bakkouri, K., Schepens, B., Roose, K., Schotsaert, M., Birkett, A., Saelens, X., (2009). M2e-based universal influenza A vaccine. *Vaccine, 27*(45), 6280-6283. doi:10.1016/j.vaccine.2009.07.007

Fierer, J. O., Veggiani, G., and Howarth, M. (2014). Spyligase peptide–peptide ligation polymerizes affibodies to enhance magnetic cancer cell capture. *Proceedings of the National Academy of Sciences, 111*(13), E1181. doi:10.1073/pnas.1315776111

Frietze, K. M., Peabody, D. S., and Chackerian, B. (2016). Engineering virus-like particles as vaccine platforms. *Current Opinion in Virology, 18*, 44-49. doi:10.1016/j.coviro.2016.03.001

Gannagé, M., Dormann, D., Albrecht, R., Dengjel, J., Torossi, T., Rämer, P. C., Münz, C. (2009). Matrix protein 2 of influenza A virus blocks autophagosome fusion with lysosomes. *Cell Host and Microbe, 6*(4), 367-380. doi:10.1016/j.chom.2009.09.005

García-Sastre, A., and Medina, R. A. (2011). Influenza A viruses: New research developments. *Nature Reviews Microbiology, 9*(8), 590-603. doi:10.1038/nrmicro2613

Godbey, W. T. (2014). In Godbey W. T. (Ed.), *Chapter 2 - proteins* Woodhead Publishing. doi.org/10.1016/B978-1-907568-28-2.00002-2

Hagan, R. M., Björnsson, R., McMahon, S. A., Schomburg, B., Braithwaite, V., Bühl, M., . . . Schwarz-Linek, U. (2010). NMR spectroscopic and theoretical analysis of a spontaneously formed lys-asp isopeptide bond. *Angewandte Chemie (International Ed. in English), 49*(45), 8421-8425. doi:10.1002/anie.201004340

Harper, D. M., De Mars, L. R. (2017). HPV vaccines – A review of the first decade. *Gynecologic Oncology, 146*(1), 196-204. doi:10.1016/j.ygyno.2017.04.004

Heinimäki, S., Tamminen, K., Malm, M., Vesikari, T., and Blazevic, V. (2017). Live baculovirus acts as a strong B and T cell adjuvant for monomeric and oligomeric protein antigens. *Virology, 511*, 114-122. doi:10.1016/j.virol.2017.08.023

Hinrichsen, M., Lenz, M., Edwards, J. M., Miller, O. K., Mochrie, S. G. J., Swain, P. S., Regan, L. (2017). A new method for post-translationally labeling proteins in live cells for fluorescence imaging and tracking. *Protein Engineering, Design and Selection : PEDS, 30*(12), 771-780. doi:10.1093/protein/gzx059

Hong, J., Chen, T., Chen, Y., Liu, C., Jan, J., and Wu, S. (2019). Highly immunogenic influenza virus-like particles containing B-cell-activating factor (BAFF) for multi-subtype vaccine development *antiviral research. vol 164: 12-22*

Houser, K., and Subbarao, K. (2015). Influenza vaccines: Challenges and solutions. *Cell Host and Microbe, 17*(3), 295-300. doi:10.1016/j.chom.2015.02.012

Huo, Y., Wan, X., Ling, T., Wu, J., Wang, W., and Shen, S. (2018). Expression and purification of norovirus virus like particles in escherichia coli and their immunogenicity in mice Molecular Immunology, 93(4), 278-284 doi://doi.org/10.1016/j.molimm.2017.07.014

Jones, M. K., Grau, K. R., Costantini, V., Kolawole, A. O., Graaf, M., Freiden, P., Karst, S. M. (2015). Human norovirus culture in B cells. *Nature Protocols, 10*(12), 1939-1947. doi:10.1038/nprot.2015.121

Kang, H. J., Coulibaly, F., Clow, F., Proft, T., and Baker, E. N. (2007). Stabilizing isopeptide bonds revealed in gram-positive bacterial pilus structure. *Science, 318*(5856), 1625-1628. doi:10.1126/science.1145806

Kang, S., Kim, M., and Compans, R. W. (2012). Virus-like particles as universal influenza vaccines. *Expert Review of Vaccines, 11*(8), 995-1007. doi:10.1586/erv.12.70

Kang, Y-k., Rha, S. Y., Tassone, P., Barriuso, J., Yu, R., Szado, T., Bang, Y-j (2014). A phase IIa dose-finding and safety study of first-line pertuzumab in combination with trastuzumab, capecitabine and cisplatin in patients with HER2-positive advanced gastric cancer. *British Journal of Cancer, 111*(4), 660-666. doi:10.1038/bjc.2014.356

Karst, S. M. (2010). and nbsp;pathogenesis of noroviruses, emerging RNA viruses and nbsp; *Viruses,* (2(3)), 748–781. Retrieved from doi:10.3390/v2030748

Koho, T., Huhti, L., Blazevic, V., Nurminen, K., Butcher, S. J., Laurinmäki, P., Kulomaa, M. S. (2012). Production and characterization of virus-like particles and the P domain protein of GII.4 norovirus. *Journal of Virological Methods, 179*(1), 1-7. doi:10.1016/j.jviromet.2011.05.009

Koho, T., Ihalainen, T. O., Stark, M., Uusi-Kerttula, H., Wieneke, R., Rahikainen, R., Hytönen, V. P. (2015). His-tagged norovirus-like particles: A versatile platform for cellular delivery and surface display. *European Journal of Pharmaceutics and Biopharmaceutics, 96*, 22-31. doi:10.1016/j.ejpb.2015.07.002

Koho, T., Koivunen, M. R. L., Oikarinen, S., Kummola, L., Mäkinen, S., Mähönen, A. J., Laitinen, O. H. (2014). Coxsackievirus B3 VLPs purified by ion exchange chromatography elicit strong immune responses in mice. *Antiviral Research, 104*, 93-101. doi:10.1016/j.antiviral.2014.01.013

Kolawole, A. O., Smith, H. Q., Svoboda, S. A., Lewis, M. S., Sherman, M. B., Lynch, G. C., Wobus, C. E. (2017). Norovirus escape from broadly neutralizing antibodies is limited to allostery-like mechanisms. *mSphere, 2*(5), 334. doi:10.1128/mSphere.00334-17

Krammer, F., Smith, G. J. D., Fouchier, Ron A. M., Peiris, M., Kedzierska, K., Doherty, P. C., Palese, P., Shaw M. L., Treanor J., Webster, R. G., and García-Sastre, A. (2018). Influenza. *Nature Reviews Disease Primers 4, Article Number: 3 (2018),*

Kumar, A., Meldgaard, T. S., and Bertholet, S. (2018). Novel platforms for the development of a universal influenza vaccine. *Front Immunol.,* 23(9), 600. doi:10.3389/fimmu.2018.00600

Kumlin, U., Olofsson, S., Dimock, K., and Arnberg, N. (2008). Sialic acid tissue distribution and influenza virus tropism. *Influenza and Other Respiratory Viruses, 2*(5), 147-154. doi:10.1111/j.1750-2659.2008.00051.x

Lamrani, A., Tubert-Bitter, P., Hill, C., and Escolano, S. (2017). A benefit–risk analysis of rotavirus vaccination, france, 2015. *Euro Surveillance : Bulletin Europeen Sur Les Maladies Transmissibles = European Communicable Disease Bulletin, 22*(50), 28. doi:10.2807/1560-7917.ES.2017.22.50.17-00041

Lee, Y. T., Ko, E. J., Lee, Y., Kim, K. H., Kim, M. C., Lee, Y. N., and Kang, S. M. (2018). Intranasal vaccination with M2e5x virus-like particles induces humoral and cellular immune responses conferring cross-protection against heterosubtypic influenza viruses. *PLoS One, 13*(1), e0190868. doi:10.1371/journal.pone.0190868

Łęga, T., Weiher, P., Obuchowski, M., and Nidzworski, D. (2016). Presenting influenza A M2e antigen on recombinant spores of bacillus subtilis. *PLoS One, 11*(11), e0167225. doi:10.1371/journal.pone.0167225

Levene, R. E., and Gaglia, M. M. (2018). Host shutoff in influenza A virus: Many means to an end. *Viruses, 10*(9), 475. doi:10.3390/v10090475

Li, L., Fierer, J. O., Rapoport, T. A., and Howarth, M. (2014). Structural analysis and optimization of the covalent association between SpyCatcher and a peptide tag. *Journal of Molecular Biology, 426*(2), 309-317. doi:10.1016/j.jmb.2013.10.021

Li, T., Lin, H., Zhang, Y., Li, M., Wang, D., Che, Y., Zhu, Y., Li, S., Zhang, J., Ge, S., Zhao, Q., Xia, N. (2014). Improved characteristics and protective efficacy in an animal model of *E. coli* -derived recombinant double-layered rotavirus virus-like particles. *Vaccine, 32*(17), 1921-1931. doi:10.1016/j.vaccine.2014.01.093

Lin, S., Chiu, H., Chiang, B., and Hu, Y. (2015). Development of EV71 virus-like particle purification processes. *Vaccine,* 4(33), 5966-73. doi.org/10.1016/j.vaccine.2015.04.077

Liu, Z., Zhou, H., Wang, W., Tan, W., Fu, Y., and Zhu, M. (2014). A novel method for synthetic vaccine construction based on protein assembly. *Scientific Reports, 4*(1), 7266. doi:10.1038/srep07266

Lucero, Y., Vidal, R., and O'Ryan G, M. (2018). Norovirus vaccines under development. *Vaccine* 36(36), 5435-5441. doi.org/10.1016/j.vaccine.2017.06.043

Mallagaray, A., Creutznacher, R., Dülfer, J., Mayer, P. H. O., Grimm, L. L., Orduña, J. M., Peters, T. (2019). A post-translational modification of human norovirus capsid protein attenuates glycan binding. *Nature Communications, 10*(1), 1320. Retrieved from https://www.ncbi.nlm.nih.gov/pubmed/30899001

Meder, D., and Simons, K. (2006). Lipid rafts, caveolae, and membrane traffic. *Lipid rafts and caveolae* (pp. 1-23). Weinheim, FRG: Wiley-VCH Verlag GmbH and Co. KGaA. doi:10.1002/3527608079.ch1 Retrieved from https://onlinelibrary.wiley.com/doi/abs/10.1002/3527608079.ch1

Meder, D., Moreno, M. J., Verkade, P., Vas, W. L., and Simons K. (2006). Phase coexistence and connectivity in the apical membrane of polarized epithelial cells. *Proceedings of the National Academy of Sciences of the United States of America, 103*(2), 329-334. doi:10.1073/pnas.0509885103

Mehalko, J. L., and Esposito, D. (2016). Engineering the transposition-based baculovirus expression vector system for higher efficiency protein production from insect cells. *Journal of Biotechnology, 238*, 1-8. doi:10.1016/j.jbiotec.2016.09.002

Mohsen, M. O., Zha, L., Cabral-Miranda, G., and Bachmann, M. F. (2017). Major findings and recent advances in virus–like particle (VLP)-based vaccines. *Seminars in Immunology, 34*, 123-132. doi:10.1016/j.smim.2017.08.014

Momose, F., Naito, T., Yano, K., Sugimoto, S., Morikawa, Y., and Nagata, K.(2002). Identification of Hsp90 as a stimulatory host factor involved in influenza virus RNA synthesis. *Journal of Biological Chemistry, 277*(47), 45306-45314. doi:10.1074/jbc.M206822200

Moorthy, V. S., and Ballou, W. R. (2009). Immunological mechanisms underlying protection mediated by RTS,S: *A review of the available data*. London: BioMed Central. doi:10.1186/1475-2875-8-312

Mühlmann, M., Forsten, E., Noack, S., and Büchs, J. (2017). Optimizing recombinant protein expression via automated induction profiling in microtiter plates at different temperatures. *Microbial Cell Factories,* 220(20), 125-132. doi:10.18154/RWTH-2018-221772

Nayak, D. P., Balogun, R. A., Yamada, H., Zhou, Z. H., and Barman, S. (2009). Influenza virus morphogenesis and budding. *Virus Research, 143*(2), 147-161. doi:10.1016/j.virusres.2009.05.010

Novák, P., and Havlíček, V. (2016). In Ciborowski P., Silberring J.(Eds.), 4 - protein extraction and precipitation. Boston*: Elsevier.* doi://doi.org/10.1016/B978-0-444-63688-1.00004-5

Osterholm, M. T. (2005). Preparing for the next pandemic. *The New England Journal of Medicine, 352*(18), 1839-1842. doi:10.1056/NEJMp058068

Philipps, B., Rotmann, D., Wicki, M., Mayr, L. M., and Forstner, M. (2005). Time reduction and process optimization of the baculovirus expression system for more efficient recombinant protein production in insect cells. *Protein Expr purif.* 42(1), 211-8. doi.org/10.1016/j.pep.2005.03.020

Quan, F., Lee, Y., Kim, K., Kim, M., and Kang, S. (2016). Progress in developing virus-like particle influenza vaccines. *Expert Rev Vaccines.* 15(10), 1281-93. doi:10.1080/14760584.2016.1175942

Reddington, S. C., and Howarth, M. (2015). Secrets of a covalent interaction for biomaterials and biotechnology: SpyTag and SpyCatcher. *Current Opinion in Chemical Biology, 29*, 94-99. doi:10.1016/j.cbpa.2015.10.002

Robilotti, E., Deresinski, S., and Pinsky, B. A. (2015). Norovirus. *Clinical Microbiology Reviews, 28*(1), 134-164. doi:10.1128/CMR.00075-14

Rodríguez-Limas, W. A., Sekar, K., and Tyo, K. E. (2013). Virus-like particles: The future of microbial factories and cell-free systems as platforms for vaccine development. *Curr. Opin Biotechnol.* 24(6), 1089-93. doi.org/10.1016/j.copbio.2013.02.008

Rossman, J. S., Lamb, R. A. (2010). Influenza virus assembly and budding. *Virology, 411*(2), 229-236. doi:10.1016/j.virol.2010.12.003

Russell, R. J., Kerry, P. S., Stevens, D. J., Steinhauer, D. A., Martin, S.R., Gamblin, S. J., and Skehel, J. J. (2008). Structure of influenza hemagglutinin in complex with an inhibitor of membrane fusion. *Proceedings of the National Academy of Sciences of the United States of America, 105*(46), 17736-17741. doi:10.1073/pnas.0807142105

Santi, L., Huang, Z., and Mason, H. (2006). Virus-like particles production in green plants. *Methods, 40*(1), 66-76. doi:10.1016/j.ymeth.2006.05.020

Sautto, G. A., Kirchenbaum, G. A., and Ross, T. M. (2018). Towards a universal influenza vaccine: Different approaches for one goal. *Virology Journal, 15*(1), 17-12. doi:10.1186/s12985-017-0918-y

Schnell, J. R., and Chou, J. J. (2008). Structure and mechanism of the M2 proton channel of influenza A virus. *Nature, 451*(7178), 591-595. doi:10.1038/nature06531

Shouval, D., Roggendorf, H., and Roggendorf, M. (2015). Enhanced immune response to hepatitis B vaccination through immunization with a pre-S1/pre-S2/S vaccine. *Medical Microbiology and Immunology, 204*(1), 57-68. doi:10.1007/s00430-014-0374-x

Siegmund, V., Piater, B., Zakeri, B., Eichhorn, T., Fischer, F., Deutsch, C., Kolmar, H. (2016). Spontaneous isopeptide bond formation as a powerful tool for engineering site-specific antibody-drug conjugates. *Scientific Reports, 6*(1), 39291. doi:10.1038/srep39291

Stetefeld, J., McKenna, S. A., and Patel, T. R. (2016). Dynamic light scattering: A practical guide and applications in biomedical sciences. *Biophysical Reviews, 8*(4), 409. Retrieved from https://www.ncbi.nlm.nih.gov/pubmed/28510011

Sutton, T. C., Chakraborty, S., Mallajosyula, V. V. A., Lamirande, E. W., Ganti, K., Bock, K. W., Subbarao, K. (2017). Protective efficacy of influenza group 2 hemagglutinin stem-fragment immunogen vaccines. *NPJ Vaccines, 2*(1), 35-11. doi:10.1038/s41541-017-0036-2

Szewczyk, B., Bieńkowska-Szewczyk, K., and Król, E. (2014). Introduction to molecular biology of influenza a viruses. *Acta Biochimica Polonica, 61*(3), 397. Retrieved from https://www.ncbi.nlm.nih.gov/pubmed/25180226

Trivedi, B., Valerio, C., and Slater, J. E. (2003). Endotoxin content of standardized allergen vaccines. *The Journal of Allergy and Clinical Immunology, 111*(4), 777-783. doi:10.1067/mai.2003.1338

Valkenburg, S. A., Mallajosyula, V. V. A., Li, O. T. W., Chin, A. W. H., Carnell, G., Temperton, N., Poon, L. L. M. (2016). Stalking influenza by vaccination with pre-fusion headless HA mini-stem. *Scientific Reports, 6*(1), 22666. doi:10.1038/srep22666

Van de Sandt, C E, Kreijtz, J., and Rimmelzwaan, G. F. (2012). Evasion of influenza A viruses from innate and adaptive immune responses. Basel: MDPI AG. *Viruses* 4(9), 1438-76. doi:10.3390/v4091438

Van Mechelen, M. (2011). Recent clinical experience with vaccines using MPL- and QS-21-containing adjuvant systems AU - garçon, nathalie. *Expert Review of Vaccines, 10*(4), 471-486. doi:10.1586/erv.11.29

Van Saparoea, H. B. B., Houben, D., De Jonge, M. I., Jong, W. S. P., and Luirink J. (2018). Display of recombinant proteins on bacterial outer membrane vesicles using protein ligation. *Washington: American Society for Microbiology.* doi:10.1128/AEM.02567-17

Veggiani, G., Zakeri, B., and Howarth, M. (2014). Superglue from bacteria: Unbreakable bridges for protein nanotechnology. *Trends in Biotechnology, 32*(10), 506-512. doi:10.1016/j.tibtech.2014.08.001

Wang, R., Zhi, Y., Guo, J., Li, Q., Wang, L., Yang, J., Zhang, G. (2015). Efficient purification of cell culture-derived classical swine fever virus by ultrafiltration and size-exclusion chromatography. *Frontiers of Agricultural Science and Engineering, 2*(3), 230-236. doi:10.15302/J-FASE-2015071

Wetzel, D., Rolf, T., Suckow, M., Kranz, A., Barbian, A., Chan, J., Piontek, M. (2018). Establishment of a yeast-based VLP platform for antigen presentation. *Microbial Cell Factories, 17*(1), 17. doi:10.1186/s12934-018-0868-0

White, L. J., Hardy, M. E., and Estes, M. K. (1997). Biochemical characterization of a smaller form of recombinant norwalk virus capsids assembled in insect cells. *Journal of Virology, 71*(10), 8066-8072. Retrieved from http://jvi.asm.org/content/71/10/8066.abstract

World Health Organisation. (2018). Influenza (seasonal). https://www.who.int/news-room/fact-sheets/detail/influenza-(seasonal)

World Health Organization. (2019). Eight things you need to know about pandemic influenza. https://www.who.int/news-room/feature-stories/detail/8-things-to-know-about-pandemic-influenza

Yang, M., Lai, H., Sun, H., and Chen, Q. (2017). Virus-like particles that display zika virus envelope protein domain III induce potent neutralizing immune responses in mice. *Scientific Reports.* 7679(7), 8847-8856. doi:10.1038/s41598-017-08247-9

Zakeri, B., Fierer, J. O., Celik, E., Chittock E. C., Schwarz-Linek U., Moy, V. T., and Howarth, M. (2012). Peptide tag forming a rapid covalent bond to a protein, through engineering a bacterial adhesin. *Proceedings of the National Academy of Sciences of the United States of America, 109*(12), 4347-4348. Retrieved from https://www.jstor.org/stable/41585493

Zeltins, A. (2013). Construction and characterization of virus-like particles: A review. *Molecular Biotechnology, 53*(1), 92-107. doi:10.1007/s12033-012-9598-4